

1 **Genomic analysis of natural intra-specific hybrids among Ethiopian**  
2 **isolates of *Leishmania donovani***

3

4 **James A. Cotton<sup>1\*</sup>, Caroline Durrant<sup>1</sup>, Susanne U. Franssen<sup>1</sup>, Tesfaye Gelanew<sup>3</sup>, Asrat**  
5 **Hailu<sup>3</sup>, David Mateus<sup>4</sup>, Mandy J. Sanders<sup>1</sup>, Matthew Berriman<sup>1</sup>, Petr Volf<sup>2</sup>, Michael A.**  
6 **Miles<sup>4</sup>, Matthew Yeo<sup>4\*</sup>**

7

8 <sup>1</sup>Wellcome Sanger Institute, Wellcome Genome Campus, Hinxton, United Kingdom.

9 <sup>2</sup>Department of Parasitology, Faculty of Science, Charles University, Prague, Czech Republic.

10 <sup>3</sup>Faculty of Medicine, Addis Ababa University, Addis Ababa, Ethiopia

11 <sup>4</sup>Faculty of Infectious and Tropical Diseases, London School of Hygiene and Tropical Medicine,  
12 London, United Kingdom

13

14 \*authors for correspondence. JAC: [james.cotton@sanger.ac.uk](mailto:james.cotton@sanger.ac.uk); MY:

15 [Matthew.Yeo@lshtm.ac.uk](mailto:Matthew.Yeo@lshtm.ac.uk).

16

17

18 **Abstract**

19

20 Parasites of the genus *Leishmania* (Kinetoplastida: Trypanosomatidae) cause widespread and  
21 devastating human diseases, ranging from self-healing but disfiguring cutaneous lesions to  
22 destructive mucocutaneous presentations or usually fatal visceral disease. Visceral leishmaniasis  
23 due to *Leishmania donovani* is endemic in Ethiopia where it has also been responsible for major  
24 epidemics. The presence of hybrid genotypes has been widely reported in surveys of natural  
25 populations, genetic variation reported in a number of *Leishmania* species, and the extant  
26 capacity for genetic exchange demonstrated in laboratory experiments. However, patterns of

27 recombination and evolutionary history of admixture that produced these hybrid populations  
28 remain unclear, as most of the relevant literature examines only a limited number (typically fewer  
29 than 10) genetic loci. Here, we use whole-genome sequence data to investigate Ethiopian *L.*  
30 *donovani* isolates previously characterised as hybrids by microsatellite and multi-locus  
31 sequencing. To date there is only one previous study on a natural population of *Leishmania*  
32 hybrids, based on whole-genome sequence. The current findings demonstrate important  
33 differences. We propose hybrids originate from recombination between two different lineages of  
34 Ethiopian *L. donovani* occurring in the same region. Patterns of inheritance are more complex  
35 than previously reported with multiple, apparently independent, origins from similar parents that  
36 include backcrossing with parental types. Analysis indicates that hybrids are representative of at  
37 least three different histories. Furthermore, isolates were highly polysomic at the level of  
38 chromosomes with startling differences between parasites recovered from a recrudescence  
39 infection from a previously treated individual. The results demonstrate that recombination is a  
40 significant feature of natural populations and contributes to the growing body of evidence  
41 describing how recombination, and gene flow, shape natural populations of *Leishmania*.

42

### 43 **Author Summary**

44

45 Leishmaniasis is a spectrum of diseases caused by the protozoan parasite *Leishmania*. It is  
46 transmitted by sandfly insect vectors and is responsible for an enormous burden of human  
47 suffering. In this manuscript we examine *Leishmania* isolates from Ethiopia that cause the most  
48 serious form of the disease, namely visceral leishmaniasis, which is usually fatal without  
49 treatment. Historically the general view was that such parasites reproduce clonally, so that their  
50 progeny are genetically identical to the founding cells. This view has changed over time and it is  
51 increasingly clear that recombination between genetically different *Leishmania* parasites occurs.  
52 The implication is that new biological traits such as virulence, resistance to drug treatments or the

53 ability to infect new species of sandfly could emerge. The frequency and underlying mechanism  
54 of such recombination in natural isolates is poorly understood. Here we perform a detailed whole  
55 genome analysis on a cohort of hybrid isolates from Ethiopia together with their potential parents  
56 to assess the genetic nature of hybrids in more detail. Results reveal a complex pattern of mating  
57 and inbreeding indicative of multiple mating events that has likely shaped the epidemiology of the  
58 disease agent. We also show that some hybrids have very different relative amounts of DNA  
59 (polysomy) the implications of which are discussed. Together the results contribute to a fuller  
60 understanding of the nature of genetic recombination in natural populations of *Leishmania*.

61

## 62 **Introduction**

63

64 *Leishmania* is a diverse genus of kinetoplastid protozoan parasites from the family  
65 trypanosomatidae. These parasites are best known as the cause of human and animal  
66 leishmaniasis, which is a clinically important neglected tropical disease affecting millions of people  
67 and causing a tremendous burden of mortality and morbidity (Herricks et al. 2017; Alvar et al.  
68 2012). Leishmaniasis comprises a spectrum of related diseases which, depending on the species,  
69 results in various presentations ranging from small, self-healing cutaneous lesions to widespread  
70 disseminated lesions, destructive mucosal and mucocutaneous pathology, and visceral disease  
71 that is usually fatal in the absence of effective chemotherapy (Herwaldt 1999). *Leishmania* have  
72 a digenetic (two host) life cycle involving a vertebrate host and 166 different species of  
73 phlebotomine sand fly that have been implicated as vectors (Akhoundi et al. 2016), although  
74 alternative invertebrate vectors may exist for some species (Seblova et al. 2015). Vertebrate hosts  
75 encompass a wide range of mammals or reptiles, and around 20 species of *Leishmania* have  
76 been reported to infect humans (Akhoundi et al. 2016).

77

78 Historically, the population structure of *Leishmania*, other trypanosomatids and indeed most  
79 protozoan parasites was considered to be largely clonal (Tibayrenc, Kjellberg, and Ayala 1990):  
80 the presumption was that admixture between members of the same clone, or between very  
81 closely related parasites was absent or rare, with minimal impact on population structure.  
82 However, at the time the clonal theory was first proposed, most population genetic data for  
83 trypanosomatids was based on inadequate sampling and use of low-resolution markers unlikely  
84 to detect admixture between genetic groups (Ramírez and Llewellyn 2014). Subsequently,  
85 extensive work using multilocus sequence typing and microsatellite markers has produced a  
86 foundation for understanding of the population genetics of some *Leishmania* species (Akhoundi  
87 et al. 2017; G. Schönian, Kuhls, and Mauricio 2011; Gabriele Schönian, Cupolillo, and Mauricio  
88 2012; Ramírez and Llewellyn 2014). Most natural *Leishmania* isolates have surprisingly little  
89 heterozygosity, which has been widely ascribed to extensive selfing (Rougeron et al. 2009, 2010;  
90 Kuhls et al. 2007), although aneuploidy variation could also contribute (Sterkers et al. 2014). In  
91 contrast there have also been a number of reports of heterozygous natural isolates possessing a  
92 mixture of alleles associated with different populations (Schwenkenbecher et al. 2006; Kuhls et  
93 al. 2013; Gelanew et al. 2014) and even different species (Ravel et al. 2006; Hamad et al. 2011),  
94 suggesting a hybrid origin of these isolates. There is therefore a growing body of evidence for  
95 genetic exchange between natural populations of several *Leishmania* species.

96  
97 Laboratory genetic crosses between at least two *Leishmania* species have been achieved in the  
98 sand fly vectors (Akopyants et al. 2009; Sadlova et al. 2011), and viable hybrids have been  
99 achieved between geographically disparate sources of *L. major* (Inbar et al. 2013). Here many  
100 hybrids possess genotypes consistent with classical meiosis; however, aneuploidy with recurrent  
101 triploidy and loss of heterozygosity (LOH) were also observed. Interspecific *L. major/L. infantum*  
102 crosses have also been performed with segregation of cutaneous and visceral traits (Romano et  
103 al. 2014). However, distinct male or female gametes of *Leishmania* have not been described,

104 although haploid stages of *Trypanosoma brucei* have recently been discovered in tsetse flies  
105 (Peacock et al. 2014).

106

107 The fact that *Leishmania* can undergo genetic exchange is of profound epidemiological  
108 importance. Genetic exchange may facilitate adaptation to new vectors, mammalian hosts or  
109 other ecological niches. For example, *Leishmania infantum/major* hybrids infect *Phlebotomus*  
110 *papatasi*, a non-permissive vector for *L. infantum* that is widespread in the Indian subcontinent  
111 (Volf et al. 2007). Hybrids between *L. braziliensis* and *L. peruviana* have also been implicated as  
112 agents of destructive forms of mucocutaneous leishmaniasis (Nolder et al. 2007). Genetic  
113 exchange could also lead to the spread between populations of genes associated with resistance  
114 to drugs. Reassortment can potentially affect sensitivity and specificity of diagnostic methods and  
115 hybrid vigour (heterosis) could also affect virulence or transmission potential. Such implications  
116 are particularly worrying in the context of recombination contributing to the generation of novel  
117 visceralising traits in populations previously causing only dermal symptoms, or if adaptation to  
118 new vector species allows existing visceralising parasites to become more widespread.

119

120 Genome-wide sequence data are crucial to explore fully the extent of hybridisation and to identify  
121 the mechanisms by which hybrids are formed (Twyford and Ennos 2011). Data from only a few  
122 genetic loci may be adequate for identifying hybrids if admixture is recent or the populations have  
123 not extensively interbred. However, sparse markers are less sensitive in identifying complex,  
124 infrequent or ancient admixture, where only a small fraction of the genome may derive from any  
125 one parent. These kinds of events are known to occur in microbial eukaryote pathogens (Ropars  
126 et al. 2018; McMullan et al. 2015; Desjardins et al. 2017). Being able to describe signatures of  
127 genetic exchange in detail is important as other processes can explain hybrid patterns of  
128 genotypes; for instance, parasexual processes based on fusion of cells followed by mitotic  
129 crossing-over have previously been observed in some protozoa and are well-described in fungi

130 (Ene and Bennett 2014). Parasexual recombination can also produce similar inheritance patterns  
131 and some evidence of this is seen in an experimental cross between different *Leishmania* species  
132 (Romano et al. 2014), where many progeny are also highly aneuploid. Whole-genome sequence  
133 data have been reported for only a single population of hybrid *Leishmania* from Turkey (Rogers  
134 et al. 2014). This population appears to have originated from a single hybridisation event between  
135 genetically disparate lineages within the *L. donovani* species complex. One of the parents  
136 appeared to be an *L. infantum*, but the precise parentage of this population remains unclear as  
137 no parental genotypes were isolated in the same region. While genomic patterns were consistent  
138 with meiosis they do not formally exclude the possibility of a parasexual process.

139  
140 Here we present a detailed genomic analysis of a natural hybrid population of *L. donovani*  
141 originating from Ethiopia. East African strains of *L. donovani* are particularly diverse, consisting  
142 of two main populations: one comprising strains from northern Ethiopia and Sudan, the other  
143 strains from southern Ethiopia and Kenya (Zackay et al. 2018) and correspond to the areas  
144 populated by two different major sand fly vectors – *Phlebotomus orientalis* being the main vector  
145 in northern Ethiopia and Sudan and *Phlebotomus martini* in the South – although other vectors  
146 have also been implicated (Seblova et al. 2013). These two geographically (and genetically)  
147 isolated populations of *L. donovani* in Ethiopia also differ in clinical phenotypes (Gelanew et al.  
148 2010). High inbreeding, seemingly incompatible with strict clonality, was observed in strains from  
149 northern Ethiopia. Microsatellite (Gelanew et al. 2010) and MLST markers (Gelanew et al. 2014)  
150 have confirmed the presence of sympatric putative parental genotypes and hybrid progeny  
151 genotypes of *L. donovani* in isolates from the northern population. Here, we apply whole-genome  
152 sequencing data to characterise more fully these Ethiopian *L. donovani* to confirm that isolates  
153 are true hybrids that originate from recombination between two different sympatric lineages. We  
154 reveal a complex pattern of inheritance implying multiple independent origins from similar parents,

155 and backcrossing with parental types. Extensive polysomy, at the level of chromosomes, is  
156 apparent in some hybrids, the significance of which is discussed.

157

## 158 **Results**

### 159 **Genome sequencing**

160

161 From each of 11 putative hybrid isolates, 1,600-2,300 Mb of sequence data (Illumina 100 bp  
162 paired-end reads) (Table 1) were generated. When mapped against the reference genome for  
163 Ethiopian *L. donovani* (Isolate LV9, WHO code: MHOM/ET/67/HU3, Rogers et al. 2011) these  
164 data produced at least 40-fold median coverage across the isolates. Generally, coverage was  
165 consistent across the genome, with more than 30 reads per sample covering at least 90% of the  
166 genome (Table 1). SNP calling identified an average of 75,775 SNPs between each individual  
167 isolate and the reference genome, and this was relatively consistent across the panel, varying  
168 between 63,042 and 89,636 (Table 1). In contrast to this consistency in the number of variable  
169 sites, the proportion inferred to be heterozygous varied considerably. Some isolates showed very  
170 low heterozygosity (for example LdM256, 0.015) while for others almost half of variant sites were  
171 inferred to be heterozygous (for example LdDM62, 0.468). Most isolates exhibiting low levels of  
172 heterozygosity (<0.1) were previously identified as putative parental genotypes (Gelanew et al.  
173 2014), in contrast putative hybrids showed much higher levels (>0.3); with the exception of one  
174 putative parental type (LdDM481) with heterozygosity more similar to that of parental isolates  
175 (0.267). In terms of large (>100 bp) structural variants, we observed 368 deletions, 282 inversions,  
176 169 duplications and 264 translocations. However, many of these variants do not segregate  
177 among the recent Ethiopian isolates sequenced here (see Figure S1), with most being  
178 heterozygous in all or most of these isolates (Table S1, Figure S1). A single 18 bp homozygous  
179 insertion on chromosome Ld33 was present in all of the Ethiopian isolates sequenced here, which  
180 was also present in reference strains LV9 and JPCM5 but not present in BPK282.

181

182 **Table 1: Sequencing data and summary statistics of read mapping and variant calls**

isolate	WHO name	Previous classification (Gelane et al, 2014)	Sequence reads (total Mb)	Median mapped coverage	Proportion of genome with $\geq 30x$ coverage	# of variable sites against LV9	Heterozygosity
LdDM19	MHOM/ET/2007/DM19	Possible hybrid*	21383530 (2138.3)	53	0.97	80930	0.301
LdDM20	MHOM/ET/2007/DM20	parental type A	19098154 (1909.8)	49	0.96	74749	0.024
LdDM62	MHOM/ET/2007/DM62	hybrid	19577434 (1957.7)	45	0.94	89636	0.468
LdDM256	MHOM/ET/2008/DM256	parental type B	19854188 (1985.4)	51	0.96	63042	0.015
LdDM257	MHOM/ET/2008/DM257	parental type B	23066268 (2306.6)	59	0.97	63088	0.016
LdDM259	MHOM/ET/2008/DM259	parental type B	16023002 (1602.3)	42	0.91	63209	0.028
LdDM295	MHOM/ET/2008/DM295	hybrid	20010052 (2001.0)	51	0.96	87546	0.388
LdDM297	MHOM/ET/2008/DM297	parental type A	20651456 (2065.1)	52	0.96	76530	0.072
LdDM299	MHOM/ET/2008/DM299	hybrid	22442162 (2244.2)	53	0.97	88605	0.462
LdDM481	MHOM/ET/2009/DM481	parental type B	20625354 (2062.5)	53	0.97	82728	0.267
LdDM559	MHOM/ET/2009/DM559	parental type B	18753496 (1875.3)	51	0.96	63469	0.030

183

184

185



186 **Genome-wide variation identifies distinct subgroups with different levels of**  
187 **heterozygosity**

188

189 A phylogenetic tree and principal components analysis of the SNP data suggesting that these 11  
190 isolates are divided into multiple groups, with two parental groups and at least two putative hybrid  
191 groups (Figure 1). As expected the two parental groups are composed of isolates with low  
192 heterozygosity. The first parental group, comprises LdDM259, LdDM559, LdDM257, LdDM256  
193 and the second, comprises LdDM20, LdDM297. LdDM481 is an outlier in that it is a highly  
194 heterozygous sample that forms a distinct lineage, intermediate between the two parental groups  
195 but clearly distant from the other four putative hybrid isolates (LdDM19, LdDM62, LdDM295,  
196 LdDM299). Two isolates (LdDM62 and LdDM299) isolated from the same patient (a post  
197 treatment recrudescence in an HIV patient) appear very similar on the tree and PCA. The first  
198 two principal components (PCs; Figure 1b) explain 86.32% of the variance (60.32% and 20%  
199 respectively) in the data broadly reflecting previous interpretation of these isolates as hybrids and  
200 parental genotypes, the putative hybrid isolates being intermediate between the sets of parentals.  
201 An interesting exception is LdDM481, which appears distinct from all other samples regarding the  
202 first PC, with all subsequent PCs showing similar patterns, up to PC5, where LdDM19 appears  
203 as distinct from the other isolates: however, this axis encompasses only 1.9% of the total variation  
204 in these data. In the phylogeny, inclusion of three additional reference genomes (LV9, an *L.*  
205 *donovani* isolate from an Ethiopian VL patient; JPCM5, a Spanish canine *L. infantum*, and  
206 BPK282 from a Nepalese VL case) revealed the diversity present in this Ethiopian cohort and  
207 their distant relationship to both *L. donovani* in the Indian subcontinent and *L. infantum* (Figure  
208 1a). The reference isolate LV9, originally isolated in 1967, appears to be closely related to one of  
209 the parental populations.

210

211 Chromosome copy number for each isolate was inferred from read depth and allele frequencies  
212 at heterozygous sites (see methods, Figure 2). Broadly, chromosomes across the majority of  
213 isolates were inferred to be diploid. The exception is chromosome 31, which, as usual in  
214 *Leishmania*, was inferred to be highly polysomic with at least four copies present in all isolates.  
215 Chromosomes 5, 6, 8, 20 and 35 were also observed at higher dosage, being at least trisomic in  
216 6 of the 11 isolates. Two samples stood out as being more highly polysomic than others: LdDM19  
217 was inferred to be tetrasomic at three chromosomes (13, 31 and 3), while LdDM299 was strikingly  
218 polysomic. For this isolate, allele frequency data suggested a minimum of tetrasomy across  
219 chromosomes, with half the chromosomes inferred at even higher dosage (6 pentasomic, 9  
220 hexasomic, 1 heptasomic, with chromosomes 31 and 33 octasomic).

221  
222 The high somy of LdDM299 is of particular interest given that LdDM62, the pre-treatment sample  
223 from the same HIV infected patient, has somy similar to the other hybrid isolates. These two  
224 isolates are otherwise genetically very similar, differing at only 4,484 sites across the genome  
225 (LdDM62 differs from the other hybrid isolates at 38,023 and 25,765 sites). The difference in allele  
226 frequency distribution between LdDM62 and LdDM299 is clear: for example, chromosomes 11,  
227 12 and 33 all show a clear peak in allele frequencies close to 0.5 in LdDM62 suggesting disomy  
228 (or at least an even chromosome dosage), but peaks at 0.33 and 0.67 in LdDM299, suggest a  
229 higher dosage of at least 3 copies (Figure 2b). The very high somy of other chromosomes is then  
230 inferred from the ratio of coverage (Figure 2a). We attempted to confirm the high ploidy of  
231 LdDM299 using flow cytometry to measure DNA content. Cells from the same population of cells  
232 that was sequenced were not available, but a cloned population separated from the sequenced  
233 cells by more than 8 *in vitro* passages was analysed. DNA content of these cells was suggestive  
234 of diploidy (S1 Fig), leaving some uncertainty about the precise somy of the LdDM299 isolate.  
235 During SNP-calling, the copy number of individual chromosomes is specified. We thus confirmed  
236 that our main results are insensitive to the assumed somy of the isolates by repeating most

237 analyses with genotypes called as though all isolates are diploid: in all cases the conclusions from  
238 our analyses are qualitatively the same with diploid genotypes, or genotypes called using the  
239 inferred somies.

240

#### 241 **Patterns of inheritance from putative parental populations**

242

243 Variants at many sites were shared by putatively hybrid isolates and either one or other of the  
244 parental group; with relatively few variants present only in the hybrids and not found elsewhere  
245 (Figure 3). LdDM481 was an exception, possessing a moderately high number of private variants  
246 and also sharing some different variants with the parental groups compared to other hybrids,  
247 particularly with parent B where other hybrid isolates shared substantially more variation.

248

249 To understand further the origins of the hybrid parasites, we identified SNP variants that are fixed  
250 differences between the two groups of parental parasites (excluding LdDM481) and used these  
251 as markers to identify the likely origin of variants identified in the hybrids, effectively 'painting' the  
252 hybrid isolate chromosomes by their likely ancestry under the hypothesis that these isolates  
253 originated as hybrids between the parental groups or close relatives. We identified a total of  
254 49,835 such 'parent-distinguishing SNP' sites at which the two parental populations were  
255 completely fixed for different alleles. These sites are distributed across all chromosomes. For the  
256 vast majority of sites, across all putative hybrid isolates, genotypes consisted of a combination  
257 these parental alleles (Table 2), supporting the notion that these isolates originated as hybrids  
258 between two parental types. The different categories of sites are strikingly unevenly distributed  
259 across the genomes suggestive of genome wide hybridisation (Figure 4). For some chromosomes  
260 these SNP markers appear to be uniformly inherited from a single parent or show uniform  
261 heterozygosity with one allele from each parental type. Most chromosomes, however, show  
262 multiple blocks of sequential SNPs of different origins, revealing a patchwork of blocks of different

263 ancestries. Isolate LdDM481 is an exception: the “blocky” structure visible in other isolates is not  
264 apparent, there are less than half the number of heterozygous sites of shared origin in comparison  
265 to any other hybrid isolates, and five times the number of genotypes containing alleles other than  
266 those fixed in the parental groups, although this still represented only 54 sites.

267

268 **Table 2 - Distributions of parental-distinguishing SNPs in putative hybrid isolates.** Values  
269 are numbers of sites in each isolate from each category. For polysomic chromosomes, sites with  
270 at least one allele from each parent are grouped as ‘heterozygous AB’ irrespective of dosage of  
271 A and B alleles.

272

isolate	Homozygous parent A	Homozygous parent B	Heterozygous AB	Genotype not unambiguously inferred from reads	Other genotype
LdDM19	21,171	10,419	16,633	1,602	10
LdDM62	15,600	2,103	29,779	2,343	10
LdDM295	25,482	1,429	21,032	1,880	12
LdDM299	15,868	2,036	18,571	13,352	8
LdDM481	31,104	10,271	7,400	1,006	54

273

274

275 To get a more quantitative understanding of the distribution of these parent distinguishing SNP  
276 sites in blocks inherited from each parent we developed a hidden Markov model (HMM) to assign  
277 putative ancestry for sites without parent-distinguishing SNPs. The HMM assigns every 100 bp  
278 window of the genome to three states: either homozygous 'parent A', homozygous 'parent B' or  
279 heterozygous (Figure 5a). The advantage of the HMM is that it can statistically assign windows  
280 even in the absence of any parent-distinguishing variants (or where those variants are  
281 ambiguous), under the assumption that transitions between the states occur in a regular way  
282 across the genome if there is no direct evidence of a change. The HMM assigns significantly  
283 different proportions of the genome to each category for different isolates (Figure 5a), and the  
284 uneven distribution of sites in each category across the genome is reflected in the fact that these  
285 proportions are quite different from the proportion of parent-distinguishing SNP sites assigned to  
286 each category. This model also estimates the length of 'runs' that form blocks of genome with a  
287 single inheritance pattern. The distribution of these block lengths provides information on the  
288 relative age of hybrids, as we would expect recombination to have broken down blocks from older  
289 introgression events more than recent events. Longer blocks suggest that fewer hybridisation  
290 events have occurred between admixed clones but backcrossing to parental clones or related  
291 parasites would also contribute to longer blocks. The block length distribution varies between  
292 isolates (Figure 5b): it suggests that LdDM62 and LdDM299 represent a more recent hybridisation  
293 with a 'parent B' type than any 'parent A' type, and that LdDM295 may originated from a more  
294 recent hybrid (or with fewer hybridisations) between the two parental types than LdDM19. For at  
295 least two isolates (LdDM62 and LdDM299) the inheritance is asymmetrical, in that they are  
296 inferred to have inherited different proportions of their genome from each of the parental types,  
297 suggesting that these isolates did not originate by crossing within a 'founder' hybrid population,  
298 but involved some degree of backcrossing with parent B types.

299

300

301 **Reconstructing haplotypes confirms that variants of each parental type are linked**

302

303 We used reads and read pairs to phase locally heterozygous sites that were physically close to  
304 each other in the genome into sets of variants known to be present on a single haplotype. We  
305 subsequently identified regions at which all heterozygous positions were phased in all 15 isolates,  
306 so that we have unambiguous information about the haplotypes present in these regions. We  
307 inferred haplotype phylogenies for nine such regions that were at least 3 kb long and had an  
308 average of at least 4 heterozygous sites per isolate; this included 9 of the 16 'fully phased' regions  
309 of 3 kb or longer (figure 6). All 9 blocks were on different chromosomes.

310

311 In most blocks (7 out of 9; Figure 6a-e, g, h) the two haplotypes for each of the four hybrid isolates  
312 (LdDM19, LdDM62, LdDM295 and LdDM299) cluster in different parts of the phylogeny. For 6 of  
313 these (Figure 6a-d, g, h), phylogenies show the expected pattern if the hybrid isolates originated  
314 from a simple, single hybridisation between the two parental types: a long branch of the haplotype  
315 tree separates all parent A haplotypes together with one haplotype of each of the 4 hybrids from  
316 parent B haplotypes with the second haplotype of each hybrid. In one block (Figure 6e) on  
317 chromosome 17 the two haplotypes for each hybrid isolate divide into two clusters as expected,  
318 but the two 'parent A' isolates (LdDM20 and LdDM297) appear in different clusters. In the  
319 chromosome 34 block, both haplotypes for one hybrid isolate (LdDM295) clustered with the same  
320 parental group – the parent A isolates (figure 6i). All of these haplotypes are consistent with a  
321 hybrid origin for the isolates but with a more complex history than a simple, single hybridisation  
322 between the two parental populations. This could involve further recombination either by  
323 'intercrossing' within the hybrid population or backcrossing to the parental types.

324

325 Only the final block (Figure 6f) does not support a simple hybrid origin for these isolates, as the  
326 two haplotypes for each isolate cluster together. Further rounds of crossing, with a different history

327 for LdDM19 and the other hybrid isolate, would explain the pattern at this locus. Examining the  
328 alignments for these blocks did not reveal any sign of recombination within reconstructed  
329 haplotypes, but did reveal some haplotypes in the putative hybrids that differ from either of the  
330 putative parental types - for example at the haplotype block on Ld10 all of the hybrids share one  
331 haplotype that is very similar to those in *L. infantum* JPCM5 but missing from any of the other *L.*  
332 *donovani* isolates (Figure 6b; figure 7a). Either the parent B isolates are a poor proxy for the true  
333 parental types at this locus, or the history of the hybrid isolates includes crossing with more than  
334 two parental populations.

335  
336 The pattern for LdDM481 haplotypes was more complex: in 7 out of 9 trees the two haplotypes  
337 for this isolate appear in the same cluster: twice with parent B haplotypes (figure 6g,h) although  
338 never very closely related to these; four times with parent A haplotypes (figure 6b,d,f,i). In one  
339 other case (Figure 6e) the parent A isolates are themselves non-monophyletic. At many of these  
340 loci, LdDM481 has haplotypes not present in other isolates. At two other loci (on Ld05 and Ld12;  
341 Figure 6a, c) LdDM481 is heterozygous for one haplotype not observed elsewhere and for one  
342 haplotype shared with parent A isolates and the hybrids. At the phased locus on Ld32 (Figure  
343 6h), the LdDM481 haplotype is apparently distantly related to BPK282; although closer inspection  
344 of this locus shows they are united by their lack of alleles present in other isolates rather than  
345 shared characters (Figure 7b).

346  
347 For the other “outgroup” isolates of *L. infantum* and *L. donovani*, the two haplotypes from each  
348 isolate consistently cluster together. Wherever parent A haplotypes are monophyletic, the  
349 Ethiopian LV9 isolate haplotypes group with them. Nepalese *L. donovani* BPK282 tends to group  
350 with the parent B isolates but is often clearly distinguishable from them; the position of *L. infantum*  
351 JPCM5 haplotypes on these trees is more variable.

352

### 353 **Kinetoplast (kDNA) phylogeny**

354

355 The kDNA maxicircle is homologous to the mitochondrial genome of other eukaryotic groups  
356 (Jensen and Englund 2012), and is thought to be uniparentally inherited in *Leishmania* (Akopyants  
357 et al. 2009) and trypanosomes (Turner et al. 1995). The maxicircle phylogeny (Figure 8) shows a  
358 close relationship between the hybrids, parental type A, LdDM481, and the historical reference  
359 LV9 isolate, and are phylogenetically distinct from parental B isolates. This contrasts with the  
360 nuclear phylogeny, which shows the hybrid samples as somewhat more closely related to parent  
361 A isolates but clearly intermediate between both parental groups: here, the parental A isolates do  
362 not even form a monophyletic group, with LV9 and hybrid LdDM297 clustering with one parental  
363 type. Surprisingly, the mitochondrial phylogeny suggests some divergence between LdDM299  
364 and LdDM62, despite them originating pre and post treatment from the same patient. However,  
365 supporting bootstrap values were low for all relationships in this part of the tree. The outlier isolate  
366 LdDM481 also appears less distant from the cluster comprising parental group A and hybrids than  
367 indicated from nuclear SNP variation, even though mutation rates are likely to be an order of  
368 magnitude greater for mitochondrial data than for the nuclear genome. The uncertainty in the  
369 precise relationships between isolates notwithstanding, the close relation between parental group  
370 A and the hybrid isolates suggests the hybrids uniparentally inherited parent type A mitochondrial  
371 genomes, and gives some support to the idea that these all originated from a single initial cross,  
372 although these data cannot exclude that there is some bias in the inheritance of kDNA between  
373 strains, or that this shared kDNA type reflect subsequent backcrossing rather than the original  
374 hybridisation.

375

376

377

378



379 **Discussion**

380

381 Hybridisation in *Leishmania* has now been demonstrated experimentally and is also observed in  
382 natural isolates across different species. These include multiple *L. braziliensis*-*L. peruviana*  
383 hybrids in Peru (Nolder et al. 2007), *L. infantum*-*L. major* hybrids (Volf et al. 2007) and a  
384 widespread lineage of *L. tropica* that appears to be disseminated from a recent hybridization event  
385 (Schwenkenbecher et al. 2006). However, the only previous whole genome analysis of hybrid  
386 *Leishmania* isolates identified a population from Turkey that appeared to be hybrids between a  
387 MON-1 genotype type of *L. infantum* and another member of the *L. donovani* species complex  
388 (Rogers et al. 2014). In that case, isolates appear to be generated solely from continued crossing  
389 within an initial hybrid population without back-crossing to either parental type. The genetic  
390 heritage of Ethiopian hybrids we describe here must be more complex. More specifically we  
391 propose that these isolates must have originated from more than one crossing event between  
392 similar parents. Additionally, crosses must have occurred between either different hybrids types  
393 or between hybrids and parentals subsequent to the ‘founding’ outcrossing event.

394

395 In more detail, our results are indicative of complex *L. donovani* populations in northern Ethiopia,  
396 with the relatively small number of isolates sequenced here representing at least three different  
397 histories. We find two distinct parental groups of isolates with low heterozygosities. The first  
398 parental group, comprising LdDM259, LdDM559, LdDM257, LdDM256 and the second,  
399 comprising LdDM20, LdDM297. We confirm that four of the heterozygous isolates (LdDM19,  
400 LdDM62, LdDM295 and LDM299) possess hybrid genotypes that are phylogenetically  
401 intermediate between these two parental groups. Most blocks of variants in these genomes can  
402 be interpreted as being inherited from one, or both of the parental populations. The large-scale  
403 structure of these genomes as blocks of variants of particular ancestry suggests that these are  
404 relatively recent events, at least in terms of the number of crossing-over events that have occurred

405 since. There are however substantial differences between the hybrids in that the number of  
406 variants shared by individual hybrid isolates and the parentals, and also their distribution across  
407 the genomes differs substantially.

408

409 Results are indicative of at least three different histories of crossing between parental types, and  
410 probably within the hybrid population itself, with LdDM299 and LdDM62 showing very similar  
411 patterns, while both LdDM19 and LdDM295 are distinct. Using a hidden Markov model, we  
412 estimated the lengths of blocks of sequence inferred to originate from each parental population.  
413 The distribution of sizes of contiguous sequence fragments derived from each parent was not  
414 consistent between the hybrids, probably reflecting differences in the timing of hybridization  
415 events; we expect that continued interbreeding and the accompanying crossing-over gradually  
416 broke down these blocks of ancestry. Hence, blocks inherited from parents in older crossing  
417 events have smaller stretches of continuity. Our HMM results thus gives qualitative insight into  
418 the relative age of the different events that gave rise to these hybrid isolates. Using this approach  
419 we infer that LdDM62 and LdDM299 have crossed onto a parent B like ancestor more recently  
420 than to parent A, while the ancestry of LdDM19 and LdDM295 from both parents is approximately  
421 equally old. This approach assessing length of inherited haplotypes has been previously used to  
422 gain quantitative results into the history of human populations (Pugach et al. 2011), but  
423 parameterising this kind of approach in *Leishmania* seems challenging, given the facultative  
424 nature of sexuality in this genus, and our current lack of understanding of recombination in  
425 *Leishmania*. In particular, we do not quantitative information on the mutation rate, recombination  
426 rate or even likely generation time of *Leishmania* in vivo. In all cases a greater proportion of the  
427 genomic variation was shared with the 'parent A' population, suggesting a more recent common  
428 ancestry with this population or backcrossing with this population during evolutionary history. The  
429 close relatedness between the LV9 isolate, isolated in the Humera district of Ethiopia in 1967,  
430 and one of the parental groups indicates that parental like genotypes have been present in this

431 region for extended periods of time. While the age of the hybridisation events we have described  
432 are unclear, the presence of genotypically stable “parental donors” over time may have facilitated  
433 the emergence of multiple hybrid populations. In summary, while we cannot reconstruct the  
434 precise history of this population, our data confirm that the population of *L. donovani* in Ethiopia  
435 has undergone multiple rounds of hybridisation, including more complex patterns of crossing than  
436 simple F1 hybridisation between parents or subsequent crossing within a hybrid population.

437

438 The highly heterozygous isolate LdDM481 emerged as a consistent outlier that forms a distinct  
439 lineage, intermediate between the two parental groups but also distinct from the other four  
440 putative hybrid isolates. The presence of haplotypes at a number of loci in this isolate which are  
441 not present in either parental population makes it seem unlikely that this is a very recent hybrid  
442 between the two parental groups in the current cohort. One explanation is that DM481 is simply  
443 a representative of a distinct, divergent population, which appears plausible considering the  
444 genetic diversity within *L. donovani* that has previously been identified within this region (Gelanew  
445 et al. 2010, 2014; Zackay et al. 2018). A more unlikely scenario is that DM481 has some recent  
446 common ancestry with the parent A population but less so with population B.

447

448 The multiplicity of hybrid and parental genotypes within this small sample of isolates from northern  
449 Ethiopia suggests that genetic exchange is commonplace among *L. donovani* populations  
450 transmitted by *P. orientalis*, and that resulting hybrid progeny may be widely disseminated. This  
451 complex evolution also implies that co-infection of *P. orientalis* with different *L. donovani* isolates  
452 occurs frequently, at least in this region. It is currently unknown if hybrids are most likely to emerge  
453 when a sand fly is co-infected with different *Leishmania* strains ingested in the same blood meal  
454 or subsequent feeds. For *T. brucei* there is evidence that the production of hybrid genotypes is  
455 most successful when both parental types are taken up in a single meal by the tsetse vector  
456 (Peacock, Bailey, and Gibson 2016).

457

458 The pattern of polysomy we observe across the cohort did not reflect the phylogenetic relationship  
459 between isolates or their assignment to hybrid or parental classes; this is consistent with a highly  
460 dynamic chromosome complement in *Leishmania* promastigotes described both experimentally  
461 (Sterkers et al. 2011) and in field samples, for example in *L. donovani* in the Indian subcontinent  
462 (ISC; Imamura et al., 2016). Indeed, aneuploidy patterns do not seem to strongly segregate  
463 between Ethiopian *L. donovani* populations (Zackay et al. 2018) despite the degree of nucleotide  
464 diversity identified in these samples from one region of Ethiopia alone being much higher than in  
465 the ISC. For example, the average pair of samples in the main ISC population differ at only 88.3  
466 sites whereas in the current cohort even two of the closely related ‘parent B’ isolates vary at an  
467 average of 1038 sites. Aneuploidy is known to be beneficial in allowing some single celled  
468 eukaryotes, for example *Saccharomyces* and *Candida*, to rapidly generate adaptive diversity (A.  
469 M. Selmecki et al. 2015), and likely contributes to adaptation in *Leishmania* (Mannaert et al. 2012;  
470 Prieto Barja et al. 2017). Aneuploidy is known to impact gene expression in *Leishmania*  
471 promastigotes (Dumetz et al. 2017; Iantorno et al. 2017). As *Leishmania* lacks classical regulation  
472 of transcription at initiation through promoters, this could contribute to parasite adaptation to at  
473 least some conditions (Laffitte et al. 2016; Mannaert et al. 2012). However, it is unclear how  
474 extensive aneuploidy variation in cultured promastigotes is relevant to the situation in either  
475 natural vectors, or in amastigotes *in vitro* or *in vivo*: while it is clear at least some variation does  
476 occur in both (Dumetz et al. 2017; Kumar et al. 2013) it appears to be much less widespread than  
477 in *in vitro* culture.

478

479 A striking result is that the sequence data suggests that isolate LdDM299, a recrudescence infection  
480 (from LdDM62) taken from the same patient was remarkably polysomic across all chromosomes  
481 relative to other isolates. Previous flow cytometry measurements of DNA content were suggestive  
482 of diploidy for both strains LdDM62 and LdDM299 and all other strains in the cohort (Gelanew et

483 al. 2014) and are therefore incongruent. However a potential confounder was that the original  
484 cloned line that was sequenced was not available for cytometric analysis, with the isolate having  
485 undergone additional passages (>8). Somy in *Leishmania* can vary dramatically and rapidly in  
486 culture (Lachaud et al. 2014; Dumetz et al. 2017) and prolonged *in vitro* culture is known to  
487 systematically reduce ploidy in experimentally derived *T. cruzi* (Lewis et al. 2009). Here, relative  
488 somy between chromosomes is inferred from the coverage depth of reads mapped to each  
489 chromosome, while the baseline somy is determined from the allele frequency distribution. In  
490 principle, this could be misleading if the samples sequenced were mixtures of clones with many  
491 different somy levels, and single cell approaches such as FISH or single cell sequencing would  
492 be needed to fully disentangle this (Dujardin et al. 2014). However, the differences in allele  
493 frequency distributions between LdDM62 and LdDM299 for many chromosomes is particularly  
494 striking (Figure 2b), so there are at least genuine differences in the complement of chromosomes  
495 between the sequenced isolates. The consistently high dosage of some chromosomes – most  
496 strikingly chromosome 31 – are also broadly consistent with previous reports (Rogers et al. 2011;  
497 Downing et al. 2011; Dumetz et al. 2017). Together these provide reassurance that somy  
498 inferences are correct. We speculate that the apparent remarkable differences in somy between  
499 LdDM62 and LdDM299 isolated from the same HIV patient, could be an adaptive response to  
500 either chemotherapy or suppression of the patient's immune response. SNP differences between  
501 LdM62 and LdM299 isolates were minimal, so aneuploidy variation could be a convenient  
502 mechanism to alter gene expression in response to drug pressure, as demonstrated in  
503 *Leishmania* (Mannaert et al. 2012) and conclusively in resistance of some pathogenic fungi to  
504 azole drugs (Kwon-Chung and Chang 2012; A. Selmecki, Forche, and Berman 2006).

505

506 Broadly, mitochondrial phylogenies corresponded to the expected nuclear genotypes (Figures 1  
507 and 8 respectively). These data suggest hybrids uniparentally inherited parent type A  
508 mitochondrial genomes in agreement with inheritance patterns seen previously in other

509 trypanosomatids (Messenger et al. 2012); (Satoskar and Snider 2009). There was some  
510 indication that LdDM62 and LdDM299, isolated from the same patient pre and post treatment,  
511 possessed some mitochondrial sequence diversity. However, bootstrap support was low. While  
512 all analyses support the clustering of LV9, parent A and hybrid isolates, the precise placement of  
513 different isolates within this cluster varied with details of the mitochondrial maxicircle assembly  
514 approach. In this context we do not interpret these small differences between nuclear and  
515 mitochondrial phylogenies as evidence of mitochondrial introgression. Mitochondrial introgression  
516 would be a very specific marker of hybridisation between populations and has been described in  
517 trypanosomatids, including *T. cruzi* (Messenger et al. 2012) and in many other organisms  
518 (Harrison and Larson 2014). Different ancestries between mitochondrial and nuclear genomes  
519 would not be expected between LdDM62 and the recrudescence infection LdDM299 in that they  
520 are likely to be the product of a single hybridisation event, based on near identical genomic  
521 structure and SNP profiles.

522

523 Current understanding regarding pattern and process of hybridisation in *Leishmania* is  
524 incomplete. Analysis of populations to detect and describe genomic variation in evolutionary  
525 recent hybrid isolates can confirm that hybridisation occurs in natural populations and provide  
526 insight into rates and patterns of recombination. For example, previous estimates based on  
527 genomic analysis from natural *L. infantum* isolates from Turkey indicate a hybridisation frequency  
528 of  $1.3 \times 10^{-5}$  meioses per mitosis (Rogers et al. 2014). However characterisation of natural systems  
529 presents particular challenges: while co-localised isolates similar to the putative parents can  
530 sometimes be found, this is not guaranteed (Rogers et al. 2014). The number of independent  
531 meioses sampled in a natural population can be small and is consistently difficult to quantify. The  
532 recent ability to derive experimental hybrids in *L. major* (Akopyants et al. 2009) and now *L.*  
533 *donovani* (Sadlova et al. 2011); Yeo et al. unpublished data) can facilitate our understanding, as  
534 multiple replicated offspring from identical (and known) parents, frequency and distribution of

535 cross-overs are easier to assess. Particular questions of interest might be to determine if  
536 recombination tends to occur at particular localised hot-spots? If so, are they associated with  
537 particular genomic features such as GC content or between polycistronic transcription units? Are  
538 crossing-over events associated with particularly high SNP mutation rates (Arbeithuber et al.  
539 2015). In the current data we do not observe particular clusters of SNPs absent in the parental  
540 populations that could suggest this, as these data have limited power to detect these effects,  
541 which would require large number of observations of independent crossing-overs between the  
542 same parental haplotypes. Similarly, the contribution of gene conversion, often associated with  
543 meiosis, on either SNPs or tandem gene families are difficult to infer in these natural data. It is  
544 also important to note that 'parental' isolates represent here are only proxies for the true parents  
545 but results are strongly suggestive of multiple recombination events in Ethiopian *L. donovani* in  
546 recent evolutionary history. Encouragingly, experiments and subsequent derivation of  
547 experimental hybrids from phylogenetically similar parental genotypes also suggest frequent  
548 recombination in different sand fly vector species (Yeo et al, unpublished data). Experimental  
549 work will produce quantitative insights to support deeper understanding of the mechanisms and  
550 implications of recombination in *L. donovani* populations.

551

552 In conclusion we have presented genome-wide sequence data for putatively hybrid isolates of *L.*  
553 *donovani* from human VL cases in Ethiopia, together with isolates possessing putative parental  
554 like genotypes. We confirmed that 4 of the 5 putative hybrids are, indeed hybrid offspring derived  
555 from strains related to these parents, but the evolutionary history of these isolates is complex:  
556 representing at least 3 different histories. The haplotypic reconstructions, distribution of parent  
557 distinguishing SNPs and patterns of allele sharing are consistent with the occurrence of more than  
558 one hybridisation event and/or intercrossing and backcrossing to parentals, which has not been  
559 observed in experimental crossing experiments to date. These data thus confirm the ability of  
560 *Leishmania* to hybridise extensively in natural populations. The population of *L. donovani* in

561 Ethiopia has undergone multiple rounds of hybridisation, and we predict complex patterns of  
562 crossing would be revealed by a more substantial sample size. Together with progress in deriving  
563 experimental hybrids there is now promise of elucidating the mechanisms and other phylo-  
564 epidemiological aspects of recombination that have widespread implications regarding the  
565 spread, diagnosis and control of *L. donovani* populations.

566

## 567 **Materials and methods**

568

569 We generated short-read paired-end sequence data for 11 isolates of *Leishmania donovani* from  
570 Ethiopia (see table 1). Full details of the origin and isolation of the strains used are described  
571 elsewhere (Gelanew et al. 2010, 2014). Briefly, all were visceral leishmania isolated between  
572 2007 and 2009 from humans in northern Ethiopia. Of note, isolate DM299 was a relapse of DM62  
573 isolated from a HIV infected patient post treatment (Libo Kemkem-Abdurafi).

574

575 DNA library preparation was performed by shearing genomic DNA into 400–600 base pair  
576 fragments by focused ultrasonication (Covaris Adaptive Focused Acoustics technology; AFA Inc.,  
577 Woburn, USA), standard multiplex Illumina libraries were prepared using the NEBNext DNA  
578 Library Kit. The libraries were amplified with 8 cycles of PCR using Kapa HiFi DNA polymerase<sup>1</sup>  
579 and were then pooled. 100bp paired-end reads were generated on the Illumina HiSeq 2000 v3  
580 according to the manufacturer's standard sequencing protocol. All sequencing data for these  
581 isolates are available from the ENA under project ERP106107. The LV9 strain  
582 (MHOM/ET/67/HU3 also known as MHOM/ET/67/L82) was originally isolated from a VL case in  
583 the Humera district in the far North of Ethiopia in 1967 (Bradley and Kirkley 1977). The JPCM5  
584 strain (MCAN/ES/98/LLM877) is an *L. infantum* from Spain, isolated from a dog in 1998; BPK282  
585 (MHOM/NP/03/BPK282/0cl2) was isolated from a human VL case in Nepal in 2003. Illumina  
586 whole-genome data for these isolates were obtained from the ENA database, with parasite



587 material, sequencing approach and analysis of these data detailed in (Rogers et al. 2011) for  
588 JPCM5 and LV9, (Downing et al. 2011) for BPK282.

589

590 Reads for each isolate were mapped to the *L. donovani* LV9 reference assembly using SMALT  
591 v0.7.0.1 (Ponstigl 2010), indexing every second 13-mer (DePristo et al. 2011) and mapping  
592 repetitively with a minimum identity of 80% and maximum insert size of 1200bp, and mapping  
593 each read in the pair independently (-x flag). Variants were called using the HaplotypeCaller  
594 algorithm of Genome Analysis Toolkit v3.4 (DePristo et al. 2011), following best-practice  
595 guidelines (Van der Auwera et al. 2013) except as detailed below. Variant calls were first filtered  
596 to remove any overlapping with a mask generated with the GEM mappability tool (Marco-Sola et  
597 al. 2012) to identify non-unique 100bp sequences and to remove 100bp either side of any gaps  
598 within scaffolds. Subsequent filtering with the Genome Analysis Toolkit removed sites using the  
599 filtering parameters:  $DP \geq 5 * ploidy$ ,  $DP \leq 1.75 * (\text{chromosome median read depth})$ ,  $FS \leq 13.0$   
600 or missing,  $SOR \leq 3.0$  or missing,  $ReadPosRankSum \leq 3.1$  AND  $ReadPosRankSum \geq -3.1$ ,  
601  $BaseQRankSum \leq 3.1$  AND  $BaseQRankSum \geq -3.1$ ,  $MQRankSum \leq 3.1$  AND  $MQRankSum$   
602  $\geq -3.1$ ,  $ClippingRankSum \leq 3.1$  AND  $ClippingRankSum \geq -3.1$ . Calls were made both  
603 assuming diploid genotypes for every chromosome across isolates, and using a somy estimated  
604 for each chromosome independently for each isolates. Somy was estimated using the EM  
605 approach described previously (Iantorno et al. 2017), and values checked by manual inspection  
606 of read depth and allele frequency data.

607

608 The whole-genome phylogeny and principal components analysis presented here were generated  
609 by using VCFtools v0.1.15 (Danecek et al. 2011) to convert the variants from GATK vcf format to  
610 the input format for plink, and then plink v1.90b3v (Purcell et al. 2007) was used for the principal  
611 components analysis and to generate pairwise distances (1 - identity by similarity). The pairwise  
612 distances were used to calculate a neighbour-joining phylogeny using the neighbor program from

613 phylip v3.6.9 (Felsenstein 2005). Phasing was based on identifying illumina reads and read pairs  
614 linking heterozygous sites within each isolate, using the phase command in samtools v.0.1.19-  
615 44428cd (Li et al. 2009), with a block size (k) of 15; the phasing results did not differ for other  
616 values of k tested (11, 13, or 20) except k=30, where few variants were phased and no blocks >  
617 1kb were shared by all isolates. Note that this phasing approach identifies heterozygous sites *de*  
618 *novo* from read mapping data rather than using the variant calls, and reconstructs at most two  
619 haplotypes at any locus. Phylogenies for the inferred haplotypes were generated using raxmlHPC  
620 v8.2.8 (Stamatakis 2014) under a GTR+I+G model of nucleotide substitution and otherwise  
621 default parameters.

622

623 Parent-distinguishing sites were identified as those for which both parent A isolates shared an  
624 identical homozygous genotype and all four parent B isolates were homozygous for a different  
625 allele. These sites could be unambiguously assigned as being derived from one or other parent  
626 in the putative hybrid isolates, assuming these other isolates were hybrids of these parents. To  
627 extend this analysis to other sites across the genome, a Hidden Markov model (HMM) was used  
628 to classify every 100bp window along the genome of the 5 suspected hybrid isolates by likely  
629 ancestry. Three hidden ancestry states (homozygous parent A, homozygous parent B and  
630 heterozygous from each parent) were used to explain the pattern across the genome of 4  
631 observed parent-distinguishing SNP “symbols” (homozygous A, homozygous B, heterozygous  
632 and a non-determinate symbol for windows with either no parent-distinguishing SNPs or more  
633 than one state). The 100bp window size was chosen to make the HMM computationally tractable  
634 and so that almost every window (198,679 out of 202,940 across 5 isolates) was unambiguous  
635 for the observed symbol. All transitions between hidden states were allowed, but each hidden  
636 state could emit only the corresponding observation or the non-determinate symbol. Initial  
637 transition and emission probabilities and trained parameters are shown in Supplementary table  
638 2; the trained parameters did not depend strongly on the initial parameters. The HMM was trained

639 independently on each chromosome and isolate, and then average transition and emission  
640 parameters, weighted by chromosome lengths used to infer hidden states. Training and Viterbi  
641 decoding of the HMM was performed using the HMM package in R v3.3.0 (R core team 2016).

642

643 kDNA maxicircle genome sequences were generated by mapping illumina sequence data against  
644 the available maxicircle sequence assembly for *L. tarentolae* (Simpson et al. 1987) and using  
645 MITObim (Hahn, Bachmann, and Chevreur 2013) to perform iterative guided assembly with block  
646 size (k parameter) of 61 and with read trimming. This produced assemblies of between 19,611bp  
647 and 21,682bp in a single contig in each isolate (the *L. tarentolae* maxicircle is 20,992bp), including  
648 the entire transcribed region: tests using less strict criteria for assembly produced longer but less  
649 reliable assemblies. The assembled contigs were then rotated using CSA (Fernandes, Pereira,  
650 and Freitas 2009) before aligning with MAFFT v7.205 (Kato and Standley 2013) with automated  
651 algorithm choice (--automated1 flag); the alignment was then trimmed with trimAl v1.4  
652 (Fernandes, Pereira, and Freitas 2009; Capella-Gutiérrez, Silla-Martínez, and Gabaldón 2009).  
653 A maximum-likelihood phylogeny was inferred using raxmlHPC v8.2.8 under a GTR+I+G model  
654 of nucleotide substitutions (Stamatakis 2014) with 10 random addition-sequence replicates, and  
655 confidence in branches of the tree assessed with 500 bootstrap replicates.

656

657

658

659

## 660 **Acknowledgements**

661 We thank the Wellcome Sanger Institute staff of the DNA pipelines at WSI for sequencing and  
662 generating sequencing libraries.

663

664

665 **References**

666

667 Akhoundi, Mohammad, Tim Downing, Jan Votýpka, Katrin Kuhls, Julius Lukeš, Arnaud Cannet,  
668 Christophe Ravel, et al. 2017. “Leishmania Infections: Molecular Targets and Diagnosis.”  
669 *Molecular Aspects of Medicine* 57 (October): 1–29.

670 Akhoundi, Mohammad, Katrin Kuhls, Arnaud Cannet, Jan Votýpka, Pierre Marty, Pascal  
671 Delaunay, and Denis Sereno. 2016. “A Historical Overview of the Classification, Evolution,  
672 and Dispersion of Leishmania Parasites and Sandflies.” *PLoS Neglected Tropical Diseases*  
673 10 (3): e0004349.

674 Akopyants, Natalia S., Nicola Kimblin, Nagila Secundino, Rachel Patrick, Nathan Peters, Phillip  
675 Lawyer, Deborah E. Dobson, Stephen M. Beverley, and David L. Sacks. 2009.  
676 “Demonstration of Genetic Exchange during Cyclical Development of Leishmania in the  
677 Sand Fly Vector.” *Science* 324 (5924): 265–68.

678 Alvar, Jorge, Iván D. Vélez, Caryn Bern, Mercé Herrero, Philippe Desjeux, Jorge Cano, Jean  
679 Jannin, Margriet den Boer, and WHO Leishmaniasis Control Team. 2012. “Leishmaniasis  
680 Worldwide and Global Estimates of Its Incidence.” *PloS One* 7 (5): e35671.

681 Arbeithuber, Barbara, Andrea J. Betancourt, Thomas Ebner, and Irene Tiemann-Boege. 2015.  
682 “Crossovers Are Associated with Mutation and Biased Gene Conversion at Recombination  
683 Hotspots.” *Proceedings of the National Academy of Sciences of the United States of*  
684 *America* 112 (7): 2109–14.

685 Bradley, D. J., and J. Kirkley. 1977. “Regulation of Leishmania Populations within the Host. I.  
686 the Variable Course of Leishmania Donovanii Infections in Mice.” *Clinical and Experimental*  
687 *Immunology* 30 (1): 119–29.

688 Capella-Gutiérrez, Salvador, José M. Silla-Martínez, and Toni Gabaldón. 2009. “trimAl: A Tool  
689 for Automated Alignment Trimming in Large-Scale Phylogenetic Analyses.” *Bioinformatics*  
690 25 (15): 1972–73.

- 691 Danecek, Petr, Adam Auton, Goncalo Abecasis, Cornelis A. Albers, Eric Banks, Mark A.  
692 DePristo, Robert E. Handsaker, et al. 2011. "The Variant Call Format and VCFtools."  
693 *Bioinformatics* 27 (15): 2156–58.
- 694 DePristo, Mark A., Eric Banks, Ryan Poplin, Kiran V. Garimella, Jared R. Maguire, Christopher  
695 Hartl, Anthony A. Philippakis, et al. 2011. "A Framework for Variation Discovery and  
696 Genotyping Using next-Generation DNA Sequencing Data." *Nature Genetics* 43 (5): 491–  
697 98.
- 698 Desjardins, Christopher A., Charles Giamberardino, Sean M. Sykes, Chen-Hsin Yu, Jennifer L.  
699 Tenor, Yuan Chen, Timothy Yang, et al. 2017. "Population Genomics and the Evolution of  
700 Virulence in the Fungal Pathogen *Cryptococcus Neoformans*." *Genome Research* 27 (7):  
701 1207–19.
- 702 Downing, Tim, Hideo Imamura, Saskia Decuypere, Taane G. Clark, Graham H. Coombs, James  
703 A. Cotton, James D. Hilley, et al. 2011. "Whole Genome Sequencing of Multiple *Leishmania*  
704 *Donovani* Clinical Isolates Provides Insights into Population Structure and Mechanisms of  
705 Drug Resistance." *Genome Research* 21 (12): 2143–56.
- 706 Dujardin, Jean-Claude, An Mannaert, Caroline Durrant, and James A. Cotton. 2014. "Mosaic  
707 Aneuploidy in *Leishmania*: The Perspective of Whole Genome Sequencing." *Trends in*  
708 *Parasitology* 30 (12): 554–55.
- 709 Dumetz, F., H. Imamura, M. Sanders, V. Seblova, J. Myskova, P. Pescher, M. Vanaerschot, et  
710 al. 2017. "Modulation of Aneuploidy in *Leishmania Donovani* during Adaptation to Different  
711 In Vitro and In Vivo Environments and Its Impact on Gene Expression." *mBio* 8 (3).  
712 <https://doi.org/10.1128/mBio.00599-17>.
- 713 Ene, Iuliana V., and Richard J. Bennett. 2014. "The Cryptic Sexual Strategies of Human Fungal  
714 Pathogens." *Nature Reviews. Microbiology* 12 (4): 239–51.
- 715 Felsenstein, J. 2005. "PHYLIP (Phylogeny Inference Package) Version 3.6."
- 716 Fernandes, Francisco, Luísa Pereira, and Ana T. Freitas. 2009. "CSA: An Efficient Algorithm to

- 717 Improve Circular DNA Multiple Alignment.” *BMC Bioinformatics* 10 (July): 230.
- 718 Gelanew, Tesfaye, Asrat Hailu, Gabriele Schönian, Michael D. Lewis, Michael A. Miles, and  
719 Matthew Yeo. 2014. “Multilocus Sequence and Microsatellite Identification of Intra-Specific  
720 Hybrids and Ancestor-like Donors among Natural Ethiopian Isolates of *Leishmania*  
721 *Donovani*.” *International Journal for Parasitology* 44 (10): 751–57.
- 722 Gelanew, Tesfaye, Katrin Kuhls, Zewdu Hurissa, Teklu Weldegebreal, Workagegnehu Hailu,  
723 Aysheshm Kassahun, Tamrat Abebe, Asrat Hailu, and Gabriele Schönian. 2010. “Inference  
724 of Population Structure of *Leishmania* *Donovani* Strains Isolated from Different Ethiopian  
725 Visceral Leishmaniasis Endemic Areas.” *PLoS Neglected Tropical Diseases* 4 (11): e889.
- 726 Hahn, Christoph, Lutz Bachmann, and Bastien Chevreux. 2013. “Reconstructing Mitochondrial  
727 Genomes Directly from Genomic next-Generation Sequencing Reads--a Baiting and  
728 Iterative Mapping Approach.” *Nucleic Acids Research* 41 (13): e129.
- 729 Hamad, S. H., Ahmed M. Musa, Eltahir A. G. Khalil, Tamrat Abebe, Brima M. Younis, Mona E.  
730 E. Elthair, Ahmed M. EL-Hassan, Asrat Hailu, and Aldert Bart. 2011. “*Leishmania*: Probable  
731 Genetic Hybrids between Species in Sudanese Isolates.” *Journal of Microbiology and*  
732 *Antimicrobials* 3: 142–45.
- 733 Harrison, Richard G., and Erica L. Larson. 2014. “Hybridization, Introgression, and the Nature of  
734 Species Boundaries.” *The Journal of Heredity* 105 Suppl 1: 795–809.
- 735 Herricks, Jennifer R., Peter J. Hotez, Valentine Wanga, Luc E. Coffeng, Juanita A. Haagsma,  
736 María-Gloria Basáñez, Geoffrey Buckle, et al. 2017. “The Global Burden of Disease Study  
737 2013: What Does It Mean for the NTDs?” *PLoS Neglected Tropical Diseases* 11 (8):  
738 e0005424.
- 739 Herwaldt, B. L. 1999. “Leishmaniasis.” *The Lancet* 354 (9185): 1191–99.
- 740 Iantorno, Stefano A., Caroline Durrant, Asis Khan, Mandy J. Sanders, Stephen M. Beverley,  
741 Wesley C. Warren, Matthew Berriman, David L. Sacks, James A. Cotton, and Michael E.  
742 Grigg. 2017. “Gene Expression in *Leishmania* Is Regulated Predominantly by Gene

- 743 Dosage.” *mBio* 8 (5). <https://doi.org/10.1128/mBio.01393-17>.
- 744 Inbar, Ehud, Natalia S. Akopyants, Melanie Charmoy, Audrey Romano, Phillip Lawyer, Dia-Eldin  
745 A. Elnaïem, Florence Kauffmann, et al. 2013. “The Mating Competence of Geographically  
746 Diverse *Leishmania* Major Strains in Their Natural and Unnatural Sand Fly Vectors.” *PLoS*  
747 *Genetics* 9 (7): e1003672.
- 748 Jensen, Robert E., and Paul T. Englund. 2012. “Network News: The Replication of Kinetoplast  
749 DNA.” *Annual Review of Microbiology* 66: 473–91.
- 750 Katoh, Kazutaka, and Daron M. Standley. 2013. “MAFFT Multiple Sequence Alignment  
751 Software Version 7: Improvements in Performance and Usability.” *Molecular Biology and*  
752 *Evolution* 30 (4): 772–80.
- 753 Kuhls, Katrin, Elisa Cupolillo, Soraia O. Silva, Carola Schweynoch, Mariana Côrtes Boité, Maria  
754 N. Mello, Isabel Mauricio, Michael Miles, Thierry Wirth, and Gabriele Schönian. 2013.  
755 “Population Structure and Evidence for Both Clonality and Recombination among Brazilian  
756 Strains of the Subgenus *Leishmania* (*Viannia*).” *PLoS Neglected Tropical Diseases* 7 (10):  
757 e2490.
- 758 Kuhls, Katrin, Lyvia Keilonat, Sebastian Ochsenreither, Matthias Schaar, Carola Schweynoch,  
759 Wolfgang Presber, and Gabriele Schönian. 2007. “Multilocus Microsatellite Typing (MLMT)  
760 Reveals Genetically Isolated Populations between and within the Main Endemic Regions of  
761 Visceral Leishmaniasis.” *Microbes and Infection / Institut Pasteur* 9 (3): 334–43.
- 762 Kumar, Pranav, Robert Lodge, Frédéric Raymond, Jean-François Ritt, Pascal Jalaguier,  
763 Jacques Corbeil, Marc Ouellette, and Michel J. Tremblay. 2013. “Gene Expression  
764 Modulation and the Molecular Mechanisms Involved in Nelfinavir Resistance in *Leishmania*  
765 *Donovani* Axenic Amastigotes.” *Molecular Microbiology* 89 (3): 565–82.
- 766 Kwon-Chung, Kyung J., and Yun C. Chang. 2012. “Aneuploidy and Drug Resistance in  
767 Pathogenic Fungi.” *PLoS Pathogens* 8 (11): e1003022.
- 768 Lachaud, Laurence, Nathalie Bourgeois, Nada Kuk, Christelle Morelle, Lucien Crobu, Gilles

- 769 Merlin, Patrick Bastien, Michel Pagès, and Yvon Sterkers. 2014. “Constitutive Mosaic  
770 Aneuploidy Is a Unique Genetic Feature Widespread in the *Leishmania* Genus.” *Microbes  
771 and Infection / Institut Pasteur* 16 (1): 61–66.
- 772 Laffitte, Marie-Claude N., Philippe Leprohon, Barbara Papadopoulou, and Marc Ouellette. 2016.  
773 “Plasticity of the *Leishmania* Genome Leading to Gene Copy Number Variations and Drug  
774 Resistance.” *F1000Research* 5 (September): 2350.
- 775 Lewis, Michael D., Martin S. Llewellyn, Michael W. Gaunt, Matthew Yeo, Hernán J. Carrasco,  
776 and Michael A. Miles. 2009. “Flow Cytometric Analysis and Microsatellite Genotyping  
777 Reveal Extensive DNA Content Variation in *Trypanosoma Cruzi* Populations and Expose  
778 Contrasts between Natural and Experimental Hybrids.” *International Journal for  
779 Parasitology* 39 (12): 1305–17.
- 780 Li, Heng, Bob Handsaker, Alec Wysoker, Tim Fennell, Jue Ruan, Nils Homer, Gabor Marth,  
781 Goncalo Abecasis, Richard Durbin, and 1000 Genome Project Data Processing Subgroup.  
782 2009. “The Sequence Alignment/Map Format and SAMtools.” *Bioinformatics* 25 (16):  
783 2078–79.
- 784 Mannaert, An, Tim Downing, Hideo Imamura, and Jean-Claude Dujardin. 2012. “Adaptive  
785 Mechanisms in Pathogens: Universal Aneuploidy in *Leishmania*.” *Trends in Parasitology* 28  
786 (9): 370–76.
- 787 Marco-Sola, Santiago, Michael Sammeth, Roderic Guigó, and Paolo Ribeca. 2012. “The GEM  
788 Mapper: Fast, Accurate and Versatile Alignment by Filtration.” *Nature Methods* 9 (12):  
789 1185–88.
- 790 McMullan, Mark, Anastasia Gardiner, Kate Bailey, Eric Kemen, Ben J. Ward, Volkan Cevik,  
791 Alexandre Robert-Seilaniantz, et al. 2015. “Evidence for Suppression of Immunity as a  
792 Driver for Genomic Introgressions and Host Range Expansion in Races of *Albugo Candida*,  
793 a Generalist Parasite.” *eLife* 4 (February). <https://doi.org/10.7554/eLife.04550>.
- 794 Messenger, Louisa A., Martin S. Llewellyn, Tapan Bhattacharyya, Oscar Franzén, Michael D.



- 795 Lewis, Juan David Ramírez, Hernan J. Carrasco, Björn Andersson, and Michael A. Miles.  
796 2012. “Multiple Mitochondrial Introgression Events and Heteroplasmy in *Trypanosoma*  
797 *Cruzi* Revealed by Maxicircle MLST and Next Generation Sequencing.” *PLoS Neglected*  
798 *Tropical Diseases* 6 (4): e1584.
- 799 Nolder, Debbie, Norma Roncal, Clive R. Davies, Alejandro Llanos-Cuentas, and Michael A.  
800 Miles. 2007. “Multiple Hybrid Genotypes of *Leishmania* (*viannia*) in a Focus of  
801 Mucocutaneous Leishmaniasis.” *The American Journal of Tropical Medicine and Hygiene*  
802 76 (3): 573–78.
- 803 Peacock, Lori, Mick Bailey, Mark Carrington, and Wendy Gibson. 2014. “Meiosis and Haploid  
804 Gametes in the Pathogen *Trypanosoma Brucei*.” *Current Biology: CB* 24 (2): 181–86.
- 805 Peacock, Lori, Mick Bailey, and Wendy Gibson. 2016. “Dynamics of Gamete Production and  
806 Mating in the Parasitic Protist *Trypanosoma Brucei*.” *Parasites & Vectors* 9 (1).  
807 <https://doi.org/10.1186/s13071-016-1689-9>.
- 808 Ponstigl, H. 2010. “Smalt.” 2010. <https://sourceforge.net/projects/smalt/>.
- 809 Prieto Barja, Pablo, Pascale Pescher, Giovanni Bussotti, Franck Dumetz, Hideo Imamura,  
810 Darek Kedra, et al. 2017. “Haplotype Selection as an Adaptive Mechanism in the Protozoan  
811 Pathogen *Leishmania Donovanii*.” *Nature Ecology & Evolution* 1 (12): 1961–69.
- 812 Pugach, Irina, Rostislav Matveyev, Andreas Wollstein, Manfred Kayser, and Mark Stoneking.  
813 2011. “Dating the Age of Admixture via Wavelet Transform Analysis of Genome-Wide  
814 Data.” *Genome Biology* 12 (2): R19.
- 815 Purcell, Shaun, Benjamin Neale, Kathe Todd-Brown, Lori Thomas, Manuel A. R. Ferreira, David  
816 Bender, Julian Maller, et al. 2007. “PLINK: A Tool Set for Whole-Genome Association and  
817 Population-Based Linkage Analyses.” *American Journal of Human Genetics* 81 (3): 559–  
818 75.
- 819 Ramírez, Juan David, and Martin S. Llewellyn. 2014. “Reproductive Clonality in Protozoan  
820 Pathogens-Truth or Artefact?” *Molecular Ecology* 23 (17): 4195–4202.

- 821 Ravel, Christophe, Sofia Cortes, Francine Pratlong, Florent Morio, Jean-Pierre Dedet, and  
822 Lenea Campino. 2006. "First Report of Genetic Hybrids between Two Very Divergent  
823 Leishmania Species: *Leishmania Infantum* and *Leishmania Major*." *International Journal for*  
824 *Parasitology* 36 (13): 1383–88.
- 825 R core team. 2016. *R: A Language and Environment for Statistical Computing*. [https://www.R-](https://www.R-project.org/)  
826 [project.org/](https://www.R-project.org/).
- 827 Rogers, Matthew B., Tim Downing, Barbara A. Smith, Hideo Imamura, Mandy Sanders, Milena  
828 Svobodova, Petr Volf, Matthew Berriman, James A. Cotton, and Deborah F. Smith. 2014.  
829 "Genomic Confirmation of Hybridisation and Recent Inbreeding in a Vector-Isolated  
830 *Leishmania* Population." *PLoS Genetics* 10 (1): e1004092.
- 831 Rogers, Matthew B., James D. Hilley, Nicholas J. Dickens, Jon Wilkes, Paul A. Bates, Daniel P.  
832 Depledge, David Harris, et al. 2011. "Chromosome and Gene Copy Number Variation Allow  
833 Major Structural Change between Species and Strains of *Leishmania*." *Genome Research*  
834 21 (12): 2129–42.
- 835 Romano, Audrey, Ehud Inbar, Alain Debrabant, Melanie Charmoy, Phillip Lawyer, Flavia  
836 Ribeiro-Gomes, Mourad Barhoumi, et al. 2014. "Cross-Species Genetic Exchange between  
837 Visceral and Cutaneous Strains of *Leishmania* in the Sand Fly Vector." *Proceedings of the*  
838 *National Academy of Sciences of the United States of America* 111 (47): 16808–13.
- 839 Ropars, Jeanne, Corinne Maufrais, Dorothée Diogo, Marina Marcet-Houben, Aurélie Perin,  
840 Natacha Sertour, Kevin Mosca, et al. 2018. "Gene Flow Contributes to Diversification of the  
841 Major Fungal Pathogen *Candida Albicans*." *Nature Communications* 9 (1): 2253.
- 842 Rougeron, Virginie, Thierry De Meeûs, Mallorie Hide, Etienne Waleckx, Herman Bermudez,  
843 Jorge Arevalo, Alejandro Llanos-Cuentas, et al. 2009. "Extreme Inbreeding in *Leishmania*  
844 *Braziliensis*." *Proceedings of the National Academy of Sciences of the United States of*  
845 *America* 106 (25): 10224–29.
- 846 Rougeron, Virginie, Thierry De Meeûs, Sandrine Kako Ouraga, Mallorie Hide, and Anne-Laure

- 847 Bañuls. 2010. “‘Everything You Always Wanted to Know about Sex (but Were Afraid to  
848 Ask)’ in *Leishmania* after Two Decades of Laboratory and Field Analyses.” *PLoS*  
849 *Pathogens* 6 (8): e1001004.
- 850 Sadlova, Jovana, Matthew Yeo, Veronika Seblova, Michael D. Lewis, Isabel Mauricio, Petr Volf,  
851 and Michael A. Miles. 2011. “Visualisation of *Leishmania* Donovanii Fluorescent Hybrids  
852 during Early Stage Development in the Sand Fly Vector.” *PloS One* 6 (5): e19851.
- 853 Satoskar, Abhay, and Heidi Snider. 2009. “Faculty of 1000 Evaluation for Demonstration of  
854 Genetic Exchange during Cyclical Development of *Leishmania* in the Sand Fly Vector.”  
855 *F1000 - Post-Publication Peer Review of the Biomedical Literature*.  
856 <https://doi.org/10.3410/f.1159113.621459>.
- 857 Schönian, Gabriele, Elisa Cupolillo, and Isabel Mauricio. 2012. “Molecular Evolution and  
858 Phylogeny of *Leishmania*.” In *Drug Resistance in Leishmania Parasites*, 15–44.
- 859 Schönian, G., K. Kuhls, and I. L. Mauricio. 2011. “Molecular Approaches for a Better  
860 Understanding of the Epidemiology and Population Genetics of *Leishmania*.” *Parasitology*  
861 138 (4): 405–25.
- 862 Schwenkenbecher, Jan M., Thierry Wirth, Lionel F. Schnur, Charles L. Jaffe, Henk Schallig,  
863 Amer Al-Jawabreh, Omar Hamarsheh, Kifaya Azmi, Francine Pratlong, and Gabriele  
864 Schönian. 2006. “Microsatellite Analysis Reveals Genetic Structure of *Leishmania* Tropica.”  
865 *International Journal for Parasitology* 36 (2): 237–46.
- 866 Seblova, Veronika, Jovana Sadlova, Barbora Vojtkova, Jan Votypka, Simon Carpenter, Paul  
867 Andrew Bates, and Petr Volf. 2015. “The Biting Midge *Culicoides* Sonorensis (Diptera:  
868 Ceratopogonidae) Is Capable of Developing Late Stage Infections of *Leishmania* Enriettii.”  
869 *PLoS Neglected Tropical Diseases* 9 (9): e0004060.
- 870 Seblova, Veronika, Vera Volfova, Vit Dvorak, Katerina Pruzinova, Jan Votypka, Aysheshm  
871 Kassahun, Teshome Gebre-Michael, Asrat Hailu, Alon Warburg, and Petr Volf. 2013.  
872 “*Phlebotomus* Orientalis Sand Flies from Two Geographically Distant Ethiopian Localities:

- 873 Biology, Genetic Analyses and Susceptibility to Leishmania Donovanii.” *PLoS Neglected*  
874 *Tropical Diseases* 7 (4): e2187.
- 875 Selmecki, Anna, Anja Forche, and Judith Berman. 2006. “Aneuploidy and Isochromosome  
876 Formation in Drug-Resistant *Candida Albicans*.” *Science* 313 (5785): 367–70.
- 877 Selmecki, Anna M., Yosef E. Maruvka, Phillip A. Richmond, Marie Guillet, Noam Shoresh,  
878 Amber L. Sorenson, Subhajyoti De, et al. 2015. “Polyploidy Can Drive Rapid Adaptation in  
879 Yeast.” *Nature* 519 (7543): 349–52.
- 880 Simpson, L., N. Neckelmann, V. F. de la Cruz, A. M. Simpson, J. E. Feagin, D. P. Jasmer, and  
881 K. Stuart. 1987. “Comparison of the Maxicircle (mitochondrial) Genomes of *Leishmania*  
882 *Tarentolae* and *Trypanosoma Brucei* at the Level of Nucleotide Sequence.” *The Journal of*  
883 *Biological Chemistry* 262 (13): 6182–96.
- 884 Stamatakis, Alexandros. 2014. “RAxML Version 8: A Tool for Phylogenetic Analysis and Post-  
885 Analysis of Large Phylogenies.” *Bioinformatics* 30 (9): 1312–13.
- 886 Sterkers, Yvon, Lucien Crobu, Laurence Lachaud, Michel Pagès, and Patrick Bastien. 2014.  
887 “Parasexuality and Mosaic Aneuploidy in *Leishmania*: Alternative Genetics.” *Trends in*  
888 *Parasitology* 30 (9): 429–35.
- 889 Sterkers, Yvon, Laurence Lachaud, Lucien Crobu, Patrick Bastien, and Michel Pagès. 2011.  
890 “FISH Analysis Reveals Aneuploidy and Continual Generation of Chromosomal Mosaicism  
891 in *Leishmania Major*.” *Cellular Microbiology* 13 (2): 274–83.
- 892 Tibayrenc, M., F. Kjellberg, and F. J. Ayala. 1990. “A Clonal Theory of Parasitic Protozoa: The  
893 Population Structures of *Entamoeba*, *Giardia*, *Leishmania*, *Naegleria*, *Plasmodium*,  
894 *Trichomonas*, and *Trypanosoma* and Their Medical and Taxonomical Consequences.”  
895 *Proceedings of the National Academy of Sciences of the United States of America* 87 (7):  
896 2414–18.
- 897 Turner, C. M. R., G. Hide, N. Buchanan, and A. Tait. 1995. “*Trypanosoma Brucei*: Inheritance of  
898 Kinetoplast DNA Maxicircles in a Genetic Cross and Their Segregation during Vegetative

899 Growth.” *Experimental Parasitology* 80 (2): 234–41.

900 Twyford, A. D., and R. A. Ennos. 2011. “Next-Generation Hybridization and Introgression.”

901 *Heredity* 108 (3): 179–89.

902 Van der Auwera, Geraldine A., Mauricio O. Carneiro, Christopher Hartl, Ryan Poplin, Guillermo

903 del Angel, Ami Levy-Moonshine, Tadeusz Jordan, et al. 2013. “From FastQ Data to High-

904 Confidence Variant Calls: The Genome Analysis Toolkit Best Practices Pipeline.” In *Current*

905 *Protocols in Bioinformatics*, 11.10.1–11.10.33.

906 Volf, Petr, Ivana Benkova, Jitka Myskova, Jovana Sadlova, Lenea Campino, and Christophe

907 Ravel. 2007. “Increased Transmission Potential of *Leishmania major*/*Leishmania Infantum*

908 Hybrids.” *International Journal for Parasitology* 37 (6): 589–93.

909 Zackay, Arie, James A. Cotton, Mandy Sanders, Asrat Hailu, Abedelmajeed Nasereddin, Alon

910 Warburg, and Charles L. Jaffe. 2018. “Genome Wide Comparison of Ethiopian *Leishmania*

911 *Donovani* Strains Reveals Differences Potentially Related to Parasite Survival.” *PLoS*

912 *Genetics* 14 (1): e1007133.

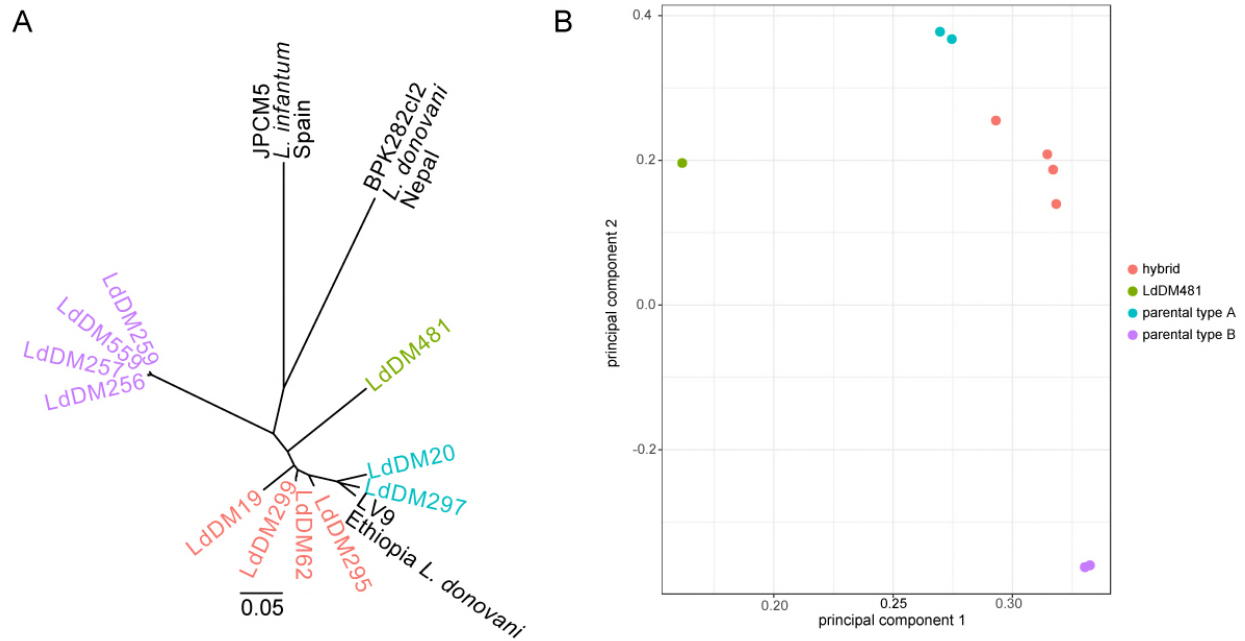
913

914

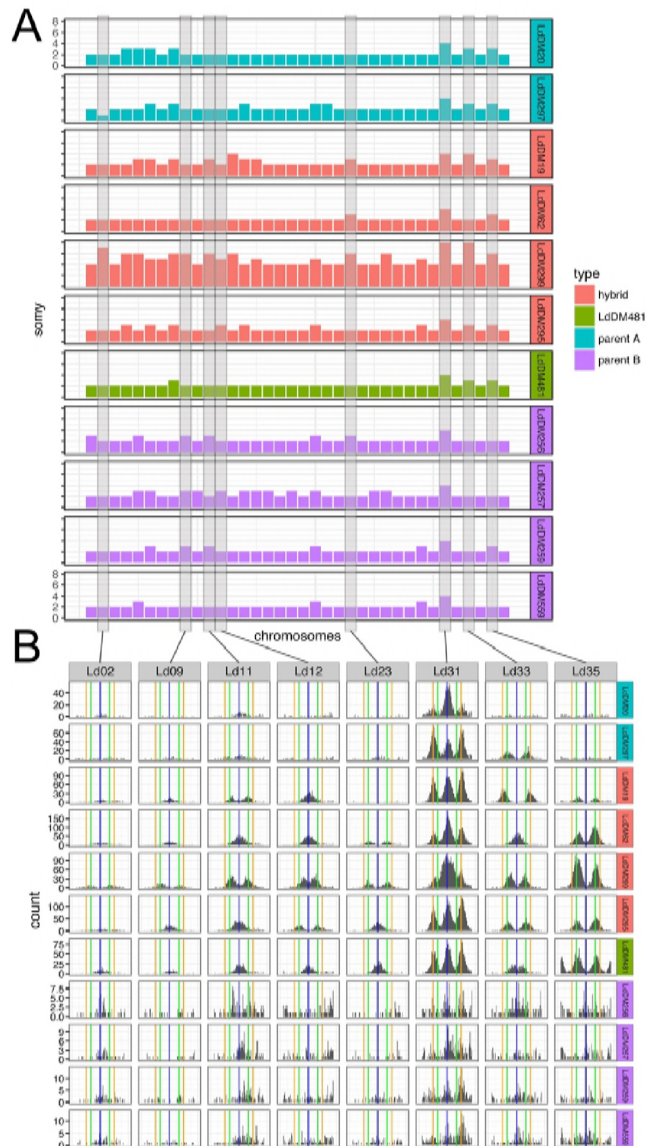
915

916 **Figures**

917



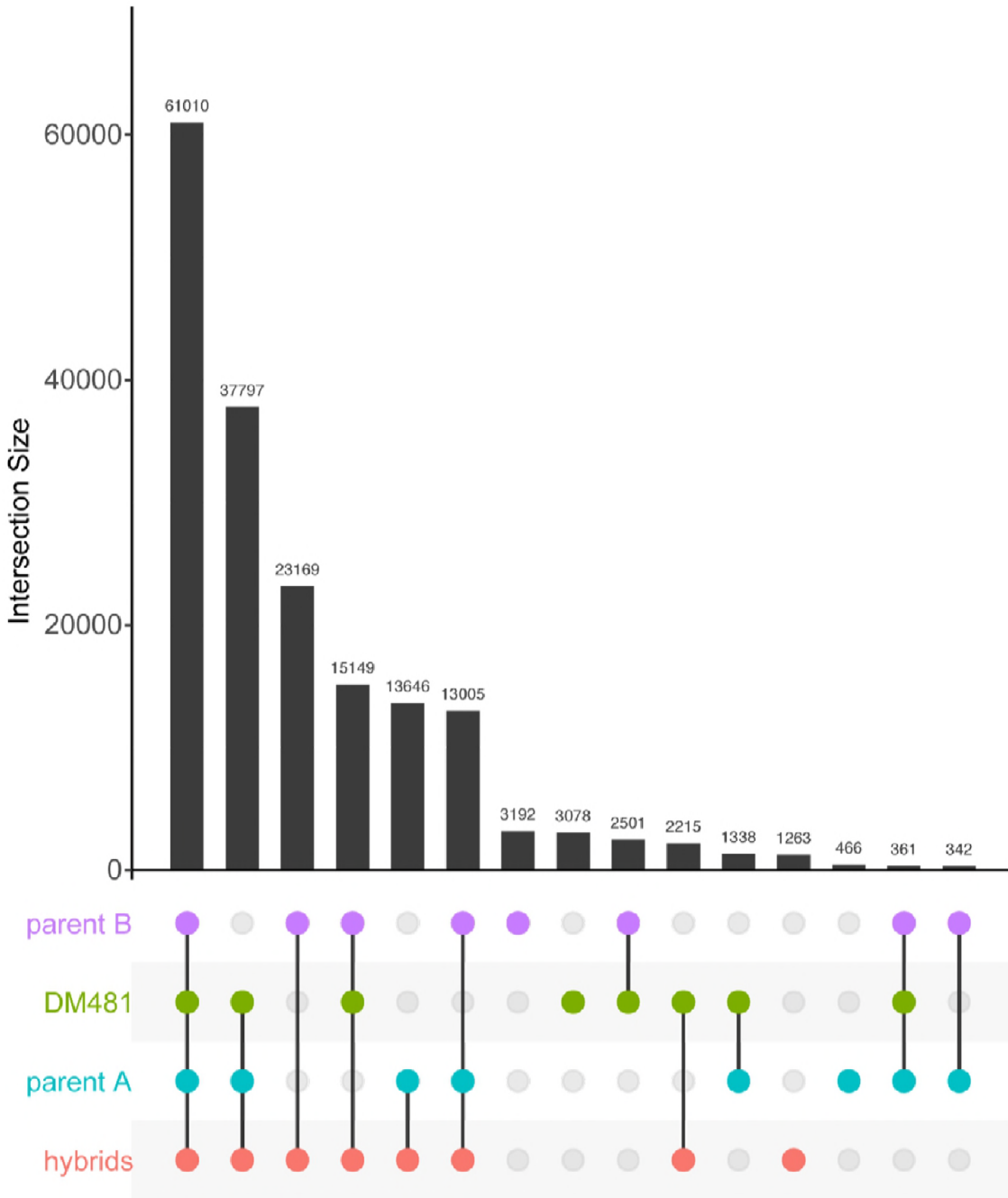
925



926

927

928 **Figure 2.** Variable somy across Ethiopian isolates inferred from coverage and allele frequencies.  
929 (A) Shows the inferred chromosome copy number (somy) for each chromosome across Ethiopian  
930 isolates under study. Y-axis scales are the same across all panel A rows. As detailed in methods,  
931 relative somy is inferred from the coverage depth of reads mapped to each chromosome, while  
932 the baseline somy is determined from the allele frequency distribution. (B) Shows example  
933 distributions of non-reference allele frequencies for each isolate, highlighting differences in somy.  
934 Vertical lines are at allele frequencies of 0.5 (blue), 0.33 and 0.67 (green), 0.25 and 0.75 (orange);  
935 expected for disomic, trisomic and tetrasomic chromosomes respectively.



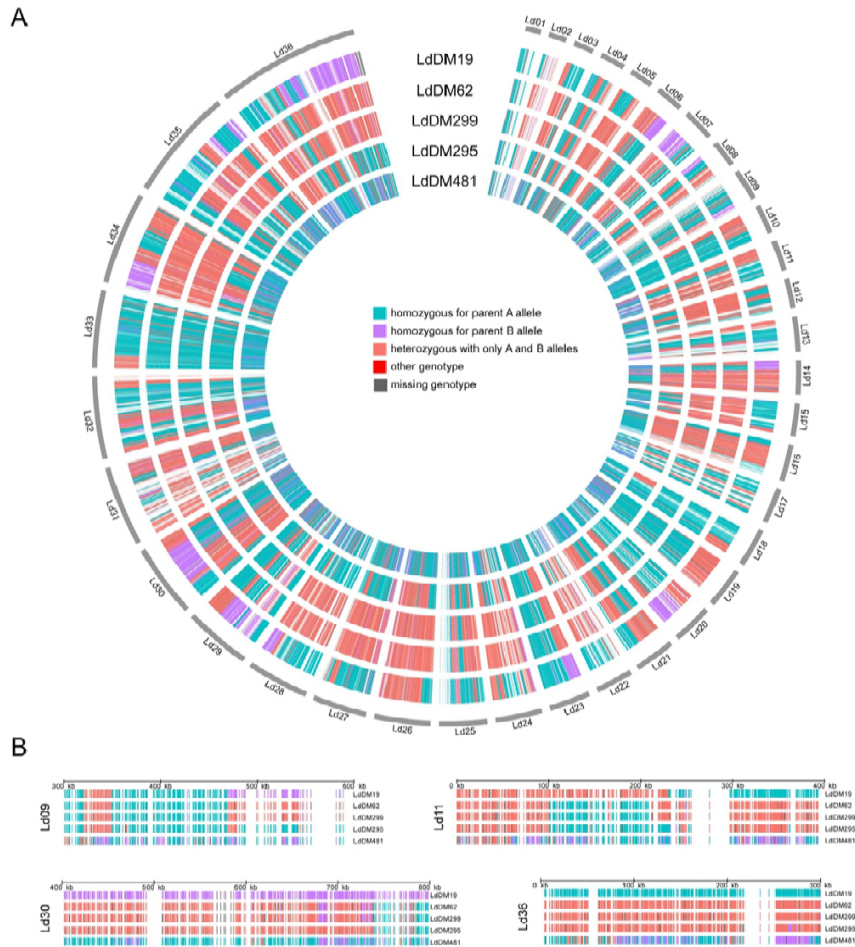
936

937 **Figure 3.** Pattern of allele sharing between groups of Ethiopian *L. donovani* isolates. Each row  
 938 corresponds to one of the categories of isolates, with columns corresponding to non-reference  
 939 alleles present in two categories or more (intersections), and the bar graph depicts the number of  
 940 alleles present in at least one of the isolates in a group for each intersection.

941

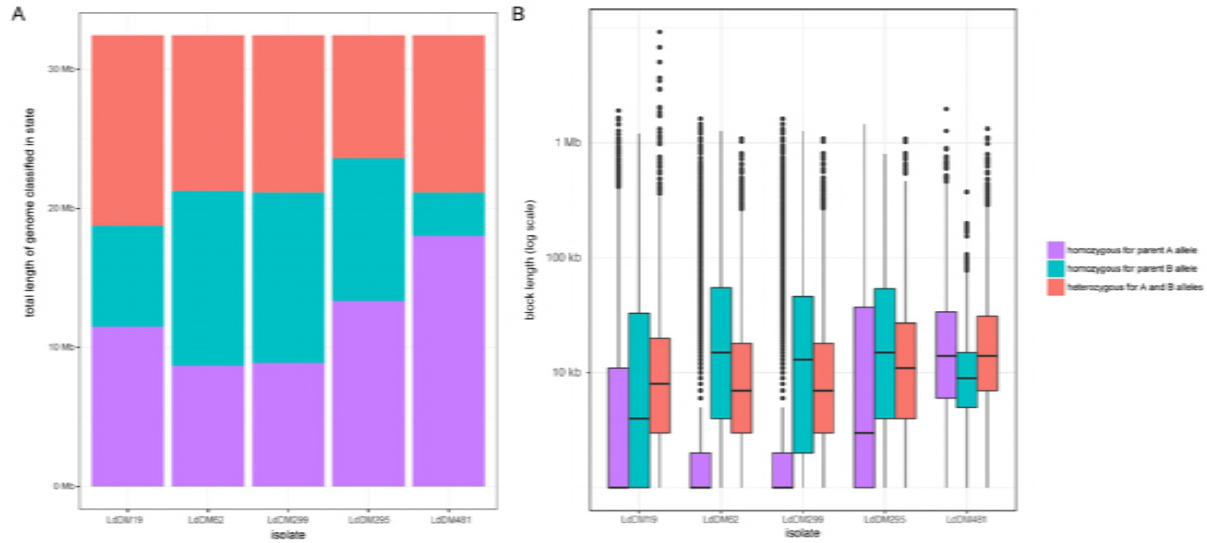
942





943

944 **Figure 4.** Distribution of SNPs distinguishing between potential parents. (A) Coloured bars in  
945 concentric rings represent every SNP that are fixed homozygous differences between the two  
946 sets of putative parents, colored to represent the diploid genotype call as homozygous for either  
947 parental type or heterozygous with one of each allele. A small number of sites had other  
948 genotypes or no reliable genotype call. There are very few SNPs in the red or grey categories.  
949 (B) Shows a magnified view of the same data for four regions, chosen to highlight variation  
950 between different isolates.



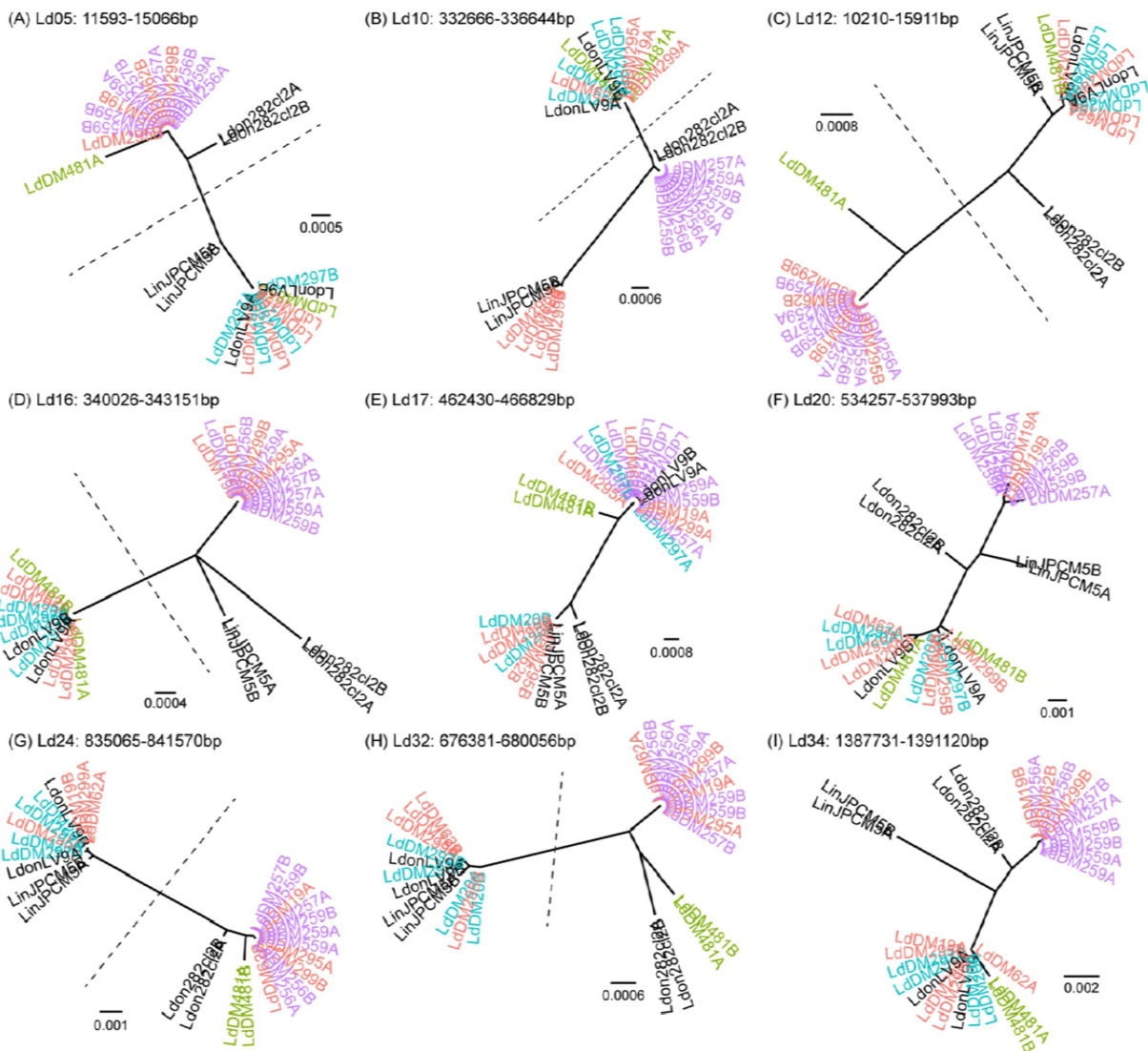
951

952 **Figure 5.** Distribution of genomic regions of putative hybrid isolates between parental origins  
953 based on Hidden Markov Model. (A) Shows the total number of basepairs assigned as  
954 homozygous parent A, homozygous parent B and heterozygous based on the maximum posterior  
955 probability assignment of hidden states of the Hidden Markov Model. (B) Box-and-whisker plot  
956 showing the distribution of lengths of contiguous blocks assigned to each of these three parentage  
957 states across the 5 putative hybrid strains in the most probable path identified in the Viterbi  
958 decoding. Boxes show median length and interquartile range on a log axis, whiskers are

959

960

961



962

963 **Figure 6.** Maximum-likelihood phylogenies for inferred haplotypes at 9 genome regions at which  
964 all isolates could be phased into blocks of length greater than 3kb and with an average of at least  
965 4 heterozygous sites per isolate. A and B labels on the leaves are arbitrary names for the two  
966 different haplotypes at each locus, for each isolate. Dotted lines separate the two hybrid  
967 haplotypes for those blocks at which all the hybrid isolates (except Ld481) have one haplotype  
968 from each putative parental population.

**(A) Ld10: 332666-336644bp**

```

LdDM257 G A G C A A G A C C T G G T G T C G T T G C C A A C T C
LdDM257 G A G C A A G A C C T G G T G T C G T T G C C A A C T C
LdDM559 G A G C A A G A C C T G G T G T C G T T G C C A A C T C
LdDM259 G A G C A A G A C C T G G T G T C G T T G C C A A C T C
LdDM559 G A G C A A G A C C T G G T G T C G T T G C C A A C T C
LdDM259 G A G C A A G A C C T G G T G T C G T T G C C A A C T C
LdDM256 G A G C A A G A C C T G G T G T C G T T G C C A A C T C
LdDM256 G A G C A A G A C C T G G T G T C G T T G C C A A C T C
Ldon282cl2 G A G C A A G A C C T G G T G T C G T T T C C A A C T C
LinJPCM5 A C A C C C A G A T C G A C A C T G A T T G C C G C A T T C
LinJPCM5 A C A C C C A G A T C G A C A C T G A T T G C C G C A T T C
Ldon282cl2 G A G C A A G A C C T G G T G T C G T T T C C A A C T C
LdDM481 G A G A A A G G C C T A G T G T C A T C T A G A A A G C C
LdonLV9 G A G A A A G G C C T A G T G T C A T C T A G A A A G C C
LdonLV9 G A G A A A G G C C T A G T G T C A T C T A G A A A G C C
LdDM481 G A G A A A G G C C T A G T G T C A T C T A G A A A G C C
LdDM299 A C A C C C A G A T C G A C A C T G A T T G C C G C A T T T
LdDM295 A C A C C C A G A T C G A C A C T G A T T G C C G C A T T T
LdDM62 A C A C C C A G A T C G A C A C T G A T T G C C G C A T T T
LdDM19 A C A C C C A G A T C G A C A C T G A T T G C C G C A T T T
LdDM19 G A G A A A G G C C T A G T G T C A T C T A G A A A G C C
LdDM299 G A G A A A G G C C T A G T G T C A T C T A G A A A G C C
LdDM295 G A G A A A G G C C T A G T G T C A T C T A G A A A G C C
LdDM295 G A G A A A G G C C T A G T G T C A T C T A G A A A G C C
LdDM62 G A G A A A G G C C T A G T G T C A T C T A G A A A G C C
LdDM20 G A G A A A G G C C T A G T G T C A T C T A G A A A G C C
LdDM297 G A G A A A G G C C T A G T G T C A T C T A G A A A G C C
LdDM297 G A G A A A G G C C T A G T G T C A T C T A G A A A G C C
LdDM20 G A G A A A G G C C T A G T G T C A T C T A G A A A G C C

```

**(B) Ld32: 676381-680056bp**

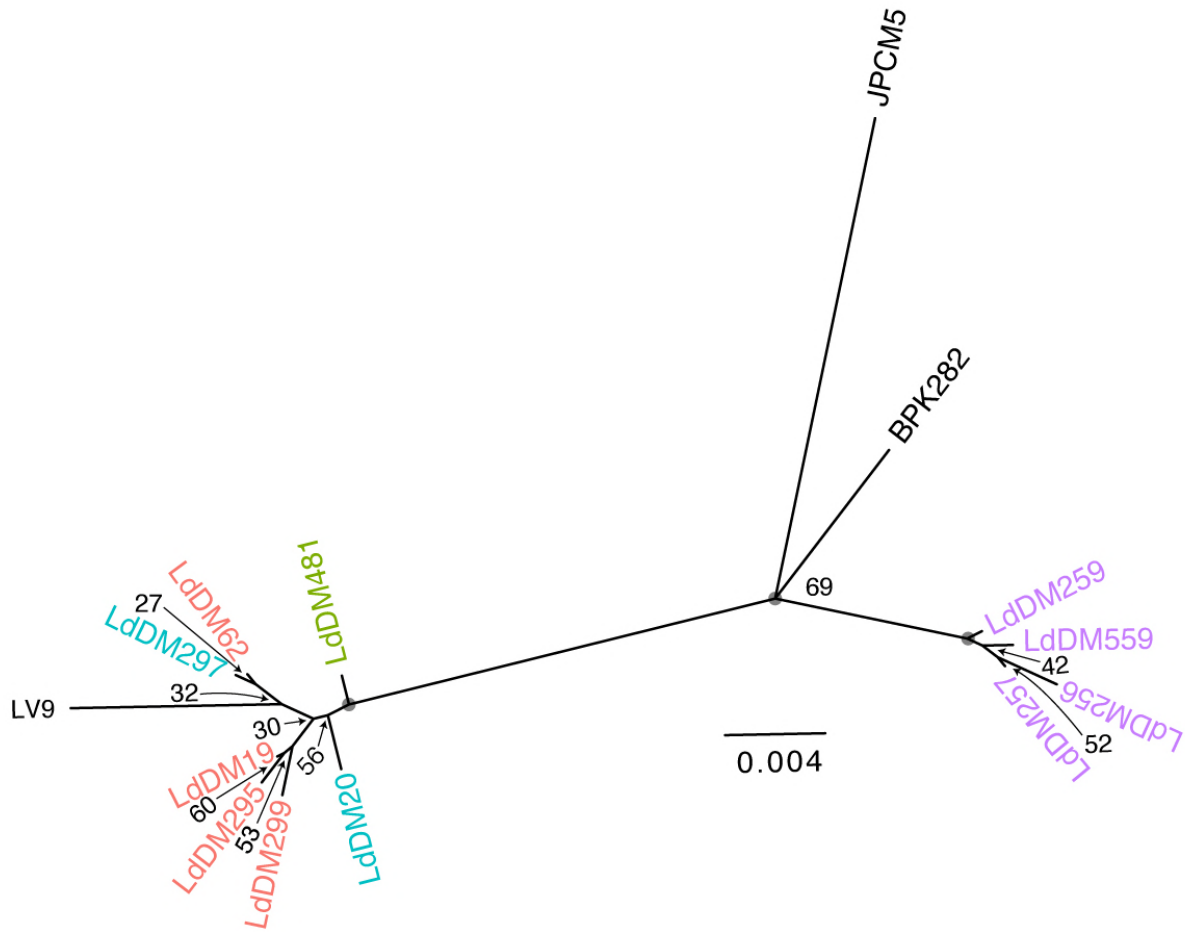
```

LdDM257 T C C C C T G A A T G G G G C G C T T T G G C A A G C T
LdDM257 T C C C C T G A A T G G G G C G C T T T G G C A A G C T
LdDM559 T C C C C T G A A T G G G G C G C T T T G G C A A G C T
LdDM259 T C C C C T G A A T G G G G C G C T T T G G C A A G C T
LdDM559 T C C C C T G A A T G G G G C G C T T T G G C A A G C T
LdDM259 T C C C C T G A A T G G G G C G C T T T G G C A A G C T
LdDM256 T C C C C T G A A T G G G G C G C T T T G G C A A G C T
LdDM256 T C C C C T G A A T G G G G C G C T T T G G C A A G C T
Ldon282cl2 T C C T A T G A G T C G A T C G T T T G G T A A T T T
Ldon282cl2 T C C T A T G A G T C G A T C G T T T G G T A A T T T
LdDM481 T T T C C T G A G C G G G T C A T T T G G C G A T T T
LdDM481 T T T C C T G A G C G G G T C A T T T G G C G A T T T
LinJPCM5 G C T C C C A A G T G A G T A G C C A A A C A G G T C
LinJPCM5 G C T C C C A A G T G A G T A G C C A A A C A G G T C
LdonLV9 G C T C C C A G G T G A G T A G C C A A A C A G G T C
LdonLV9 G C T C C C A G G T G A G T A G C C A A A C A G G T C
LdDM19 T C C C C T G A A T G G G G C G C T T T G G C A A G C T
LdDM295 T C C C C T G A A T G G G G C G C T T T G G C A A G C T
LdDM299 T C C C C T G A A T G G G G C G C T T T G G C A A G C T
LdDM62 T C C C C T G A A T G G G G C G C T T T G G C A A G C T
LdDM299 G C T C C A A G G T G A G T A G C C A A A C A G G T C
LdDM62 G C T C C A A G G T G A G T A G C C A A A C A G G T C
LdDM19 G C T C C A A G G T G A G T A G C C A A A C A G G T C
LdDM295 G C T C C A A G G T G A G T A G C C A A A C A G G T C
LdDM20 G C T C C A A G G T G A G T A G C C A A A C A G G T C
LdDM297 G C T C C C A G G T G A G T A G C C A A A C A G G T C
LdDM297 G C T C C C A G G T G A G T A G C C A A A C A G G T C
LdDM20 G C T C C C A G G T G A G T A G C C A A A C A G G T C

```

969

970 **Figure 7.** Alignments of inferred haplotypes in fully-phased regions, showing unusual haplotypes  
 971 in (a) the hybrid isolates and (b) LdDM481. Panels show all variable sites within two of the ‘fully  
 972 phased’ genome regions shown on figure 5. In all panels, red sites identify alleles specific to two  
 973 unusual haplotypes discussed in the text. Cyan and magenta identify sites at which parent A and  
 974 parent B isolates share fixed different alleles (parent distinguishing sites).



975

976 **Figure 8.** Maximum-likelihood phylogeny of reconstructed mitochondrial (kDNA maxicircle)  
977 haplotypes. Values on nodes are bootstrap support values for the partition induced by deleting  
978 the edge below each node, grey circles denote 100% support.

979

980

981 **Supplementary table 1.** Large (> 100bp) Structural variation between isolates (\* this does not  
982 include LV9).  
983

	Number of variants called	variants segregating in recent Ethiopian isolates*	Average heterozygosity in parent A isolates	Average heterozygosity in parent B isolates	Average heterozygosity in putative hybrids	Heterozygosity of Ld481	Average heterozygosity of outgroups
Duplications	169	95	0.64	0.60	0.68	0.69	0.15
Deletions	368	279	0.61	0.49	0.62	0.60	0.23
Inversions	282	147	0.63	0.56	0.69	0.65	0.17
Insertions	1	0	0	0	0	0	0
Translocations	264	123	0.44	0.36	0.42	0.44	0.16

984

985 **Supplementary table 2.** Initial transition (a) and emission (b) probability matrix and trained  
986 transition (c) and emission (d) probabilities for HMM. NA represents “Not Allowed” emissions  
987 from that state.

988

989 (a)

From \ To	A	B	Het
A	0.8	0.1	0.1
B	0.1	0.8	0.1
Het	0.05	0.05	0.9

990

991 (b)

992

State \ Symbol	A	B	Het	Non-determinate
A	0.46	NA	NA	0.54
B	NA	0.46	NA	0.54
Het	NA	NA	0.46	0.54

993

994 (c)

From \ To	A	B	Het
A	0.94105911	0.03861683	0.02032406
B	0.08776222	0.88229226	0.02994551
Het	0.04503840	0.04030465	0.91465696

995

996 (d)

997

State \ Symbol	A	B	Het	Non-determinate
A	0.1592378	NA	NA	0.8407622
B	NA	0.1653358	NA	0.8346642
Het	NA	NA	0.0878155	0.9121845

998

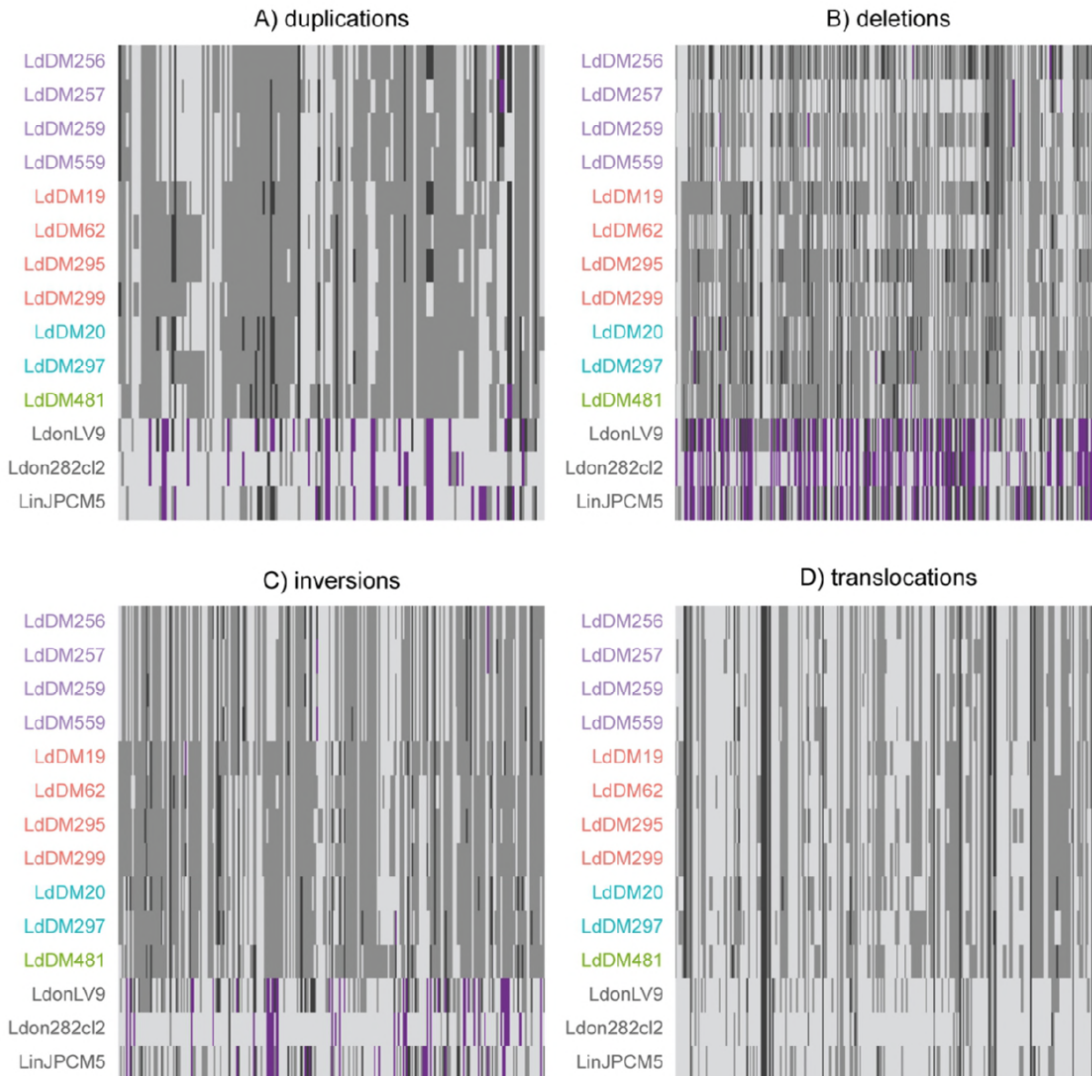
999

1000

1001

1002

1003 **Supplementary figure 1.** Overlaid DNA histograms for selected cloned *Leishmania* strains  
1004 illustrating comparable ( $2n$ ) DNA content representative of all hybrids (grey histogram) and both  
1005 parental groups (cyan and red histogram). Gates were created for G1-0 ( $2n$ ) peaks and for G2-M  
1006 ( $4n$ ) peaks. Each strain was tested in triplicate at a minimum and a control *Leishmania* strain  
1007 included in each run as an internal standard. Relative DNA content values were calculated as a  
1008 ratio compared with the internal standard. Mean G1-0 values were taken to infer relative DNA  
1009 content. The x-axes represent fluorescence intensity (arbitrary units) and the y-axes represent  
1010 number of events in each channel.  
1011



1012